

Effect of radiation on transport in graphene

S. V. Syzranov¹, M. V. Fistul¹, and K. B. Efetov^{1,2}

¹*Theoretische Physik III, Ruhr-Universität Bochum, D-44801 Bochum, Germany*

²*L. D. Landau Institute for Theoretical Physics, 119334 Moscow, Russia*

(Dated: October 27, 2018)

We study transport properties of graphene-based p-n junctions irradiated by an electromagnetic field (EF). The resonant interaction of propagating quasiparticles with external monochromatic radiation opens *dynamical gaps* in their spectrum, resulting in a strong modification of current-voltage characteristics of the junctions. The values of the gaps are proportional to the amplitude of EF. We find that the transmission of the quasiparticles in the junctions is determined by the tunneling through the gaps, and can be fully suppressed when applying a sufficiently large radiation power. However, EF can also generate current, but not only suppress it. We demonstrate that if the height of the potential barrier exceeds a half of the photon energy, the directed current (*photocurrent*) flows through the junction without any dc bias voltage applied. Such a photocurrent arises as a result of inelastic quasiparticle tunneling assisted by one- or two-photon absorption. We calculate current-voltage characteristics of diverse graphene-based junctions and estimate their parameters necessary for the experimental observation of the photocurrent and transmission suppression.

PACS numbers: 05.60.Gg, 81.05.Uw, 42.50.Hz, 73.63.-b

I. INTRODUCTION

Since its first fabrication¹, graphene, a monolayer of carbon atoms, has attracted a lot of attention as a candidate for the base material in nanoelectronics. The unique feature of this two-dimensional (2D) semiconductor is the absence of the gap between the conduction and the valence bands², which allows one to change the type of the carriers and vary their density in a wide range by applying an external gate voltage. Other outstanding properties of the material are the high carrier mobility and a submicron mean free path at room temperature^{1,3,4,5,6,7,8,9,10}. As a result, a lot of experimental activity has been devoted recently to investigation of possibilities of using graphene in the field-effect-transistor type applications^{9,11,12,13,14,15,16,17}.

In order to construct such devices one needs to be able to control and switch off currents applying gate potentials. In conventional semiconductors currents can be blocked by applying gate voltages that create sufficiently high potential barriers confining electrons in a certain region. However, the dynamics of low-energy quasiparticles in graphene is described by the zero-mass Dirac-type Hamiltonian^{18,19}, making possible their *reflectionless* transmission through potential barriers of arbitrary strength (the so-called Klein paradox)²⁰. Such an unusual phenomenon reduces the possibility to switch off currents by means of gate electrodes and is a very important property of graphene.

It is also well known for many years that the transport properties of diverse semiconducting nanostructures are sensitive to an externally applied electromagnetic field (EF). Though optoelectronic devices such as radiation-controlled field-effect transistors, photodiodes, and light-emitting diodes have been fabricated on the basis of carbon nanotubes^{21,22,23,24,25}, a little attention has been paid so far to the possibility to control and switch off

currents in graphene using external electromagnetic radiation.

In this paper we study theoretically the transport in graphene subject to a coordinate-dependent potential $U(\mathbf{r})$ and irradiated by electromagnetic field. For simplicity we assume that EF is monochromatic and linearly polarized but a proper generalization can be easily made. We show that the resonant interaction of propagating quasiparticles in graphene with EF leads to the formation of a *dynamical gap* Δ in the quasiparticle spectrum. The value of the gap depends on the intensity S and the frequency Ω of external radiation. The formation of such a dynamical gap is a generic quantum property of systems described by the two-bands Hamiltonian, and the quantity Δ/\hbar has the same meaning as the famous Rabi frequency for microwave-induced quantum coherent oscillations between two energy levels²⁶. For conventional semiconductors the dynamical gap has been predicted in the Ref. 27. Charged impurities in a sample²⁸, electron-phonon²⁹, and electron-electron interactions³⁰ smear the quasiparticle spectrum and wash out the dynamical gap. Therefore, the dynamical gap in a uniform semiconductor can be observed only if the radiation intensity exceeds some critical value S_c . Under such conditions it has been observed in the optical experiments^{31,32}.

So far only bulk properties (such as conductivity³³ and coefficient of light absorption^{27,34,35}) in absence of coordinate-dependent potentials have been studied in semiconductors with dynamical gaps. In this case an experimental observation of a dynamical gap is quite difficult and demands considerable efforts. At the same time, the question about what happens if the system is subject to an external potential has not been addressed yet.

In this paper we consider irradiated graphene junctions subject to a *non-uniform* step-like external potentials, such that the energies of conducting electrons are lo-

cated inside the dynamical gaps only in some narrow resonant regions. This means that during the transmission through the junction each electron in a large energy interval of the order of potential height has to pass through a small “classically forbidden” spatial region, where it has to move inside the gap. Thus, the current-voltage characteristics of the junctions are mainly determined by the tunneling through the gaps.

Changing the values of the gaps (i.e. the intensity and the frequency of external radiation) and the heights of potential barriers, it is possible to vary the current-voltage characteristics, e.g. to suppress Klein tunneling in graphene p-n junctions by a sufficiently strong radiation. A short account of this phenomenon has been considered recently in Ref. 36.

However, it turns out that even more interesting effect is possible in such a p-n junction. Here we demonstrate that in this system, provided the height of the potential is larger than a half of the photon energy, the directed current (*photocurrent*) flows through the junction without any dc bias voltage applied. Such a photocurrent arises as a result of inelastic quasiparticle transmission through the junction assisted by one- or two-photon absorption. We show, that in the presence of impurities and electron-electron interaction in the limit of small radiation intensities the coefficients of reflection or transmission at the resonant regions slightly differ from those in ballistic case even if the radiation intensity S is much below the critical value S_c , at which the dynamical gap vanishes. As a result, for experimentally relevant parameters of the junctions the photocurrent is not affected by elastic impurities and electron-electron interactions and, we hope, it can be observed rather easily at moderate radiation intensities.

The photocurrent we calculated for a typical graphene p-n junctions is by several orders of magnitude larger than those measured in carbon nanotubes^{22,23,24} for the same radiation intensities, since the effectively two-dimensional graphene junction has accordingly larger number of conducting channels. As there is no gap between the conduction and the valence bands in graphene, and the level of doping can be varied in a wide range using gate electrodes, graphene-based photodiode can be operated in a wide frequency range of the external radiation in the far-infrared region.

The paper is organized as follows. In Sec. II, we derive a general expression for the current flowing through the junction in presence of a monochromatic linearly polarized radiation. The current is determined by the symmetries of the Hamiltonian and the scattering matrix for the system. In order to find explicitly the scattering matrix in a spatially inhomogeneous potential in the presence of radiation one needs to know the probability of tunneling through the dynamical gap, which is calculated in Sec. III. Then, in Sec. IV, we consider electron ballistic trajectories in a p-n junction to determine how many times and where electrons tunnel during the transmission through the junction. Using these results, we

calculate in Sec. V current-voltage characteristics of irradiated ballistic graphene junctions. In Sec. VI, using the kinetic equation approach, we analyze effects of disorder and electron-electron interaction on the photocurrent in graphene p-n junctions. In Sec. VII we estimate the magnitudes of the photocurrent and the tunneling probabilities for experimentally achievable radiation intensities and parameters of the junctions.

II. CURRENT-VOLTAGE CHARACTERISTICS OF IRRADIATED BALLISTIC GRAPHENE JUNCTIONS: GENERIC ANALYSIS

In this section we derive a general expression for the current-voltage characteristics of an irradiated two-dimensional graphene strip connected to two reservoirs, from now on called the left (L) and the right (R) leads. We assume that electrons in the strip move in a coordinate-dependent potential $U(z)$, varying only along the strip, and interact with a time-periodic EF. In the present and two subsequent sections we consider a clean system, such that the transport in the strip is purely ballistic.

Another important assumption we use is that far in the leads the radiation is either absent or its effect on the electron motion and distribution functions is negligible. In the next section we show that the latter condition is satisfied since the majority of the conducting electrons in the reservoirs have their energies not too close to the positions of the radiation-induced gaps in their spectra.

Our derivation is similar to the one presented in the Ref. 37 but is adopted for the case of two-dimensional graphene strip and leads. Assume, that far in the α -th lead the electron states are plane waves, incoming to the strip, $|\varepsilon, \theta\rangle_\alpha^{in}$, or outgoing from it, $|\varepsilon, \theta\rangle_\alpha^{out}$, characterized only by the energy ε and the angle θ of incidence or scattering correspondingly. Note here, that there is no intervalley and spin scattering in a ballistic sample and thus we disregard these degrees of freedom.

According to the Floquet theorem²⁶, the general solution of the Schrödinger equation for an electron, moving in a static potential and subject to a periodic perturbation, takes the form $\Psi(t) = e^{-i\varepsilon t}\Phi_T(t)$, where $\Phi_T(t)$ is a periodic function having the same period T as the perturbation. Therefore, an electron incident with energy ε on the strip can scatter only into the states with energies $\varepsilon + n\hbar\Omega$, where $\Omega = 2\pi/T$ and $n = 0, \pm 1, \pm 2, \pm 3, \dots$, or, in other words, the particle can gain or lose only an integer number of quanta $\hbar\Omega$.

Thus, the state $|\varepsilon, \theta\rangle_\alpha^{in}$ scatters into

$$\sum_{\beta, n} \int d\phi t_{\alpha\beta}(\varepsilon, \theta; \varepsilon + n\hbar\Omega, \phi) |\varepsilon + n\hbar\Omega, \phi\rangle_\beta^{out}, \quad (2.1)$$

where we have introduced the amplitude $t_{\alpha\beta}$ of scattering from the state of an electron incident on the strip from the α -th lead at the energy ε and angle θ into the state

outgoing from the strip in the β -th lead at the energy $\varepsilon + n\hbar\Omega$ and angle ϕ . The quantity $|t_{\alpha\beta}(\varepsilon, \theta; \varepsilon + n\hbar\Omega, \phi)|^2 d\phi$ gives the probability to scatter into the angle interval $(\phi; \phi + d\phi)$.

Accordingly,

$$\sum_{\beta, n} \int d\phi |t_{\alpha\beta}(\varepsilon, \theta; \varepsilon + n\hbar\Omega, \phi)|^2 = 1. \quad (2.2)$$

In order to obtain the current flowing through the strip we introduce the distribution functions $f_{\alpha}^{in, out}(\varepsilon, \theta)$ of electrons in the incoming/outgoing states of the α -th lead. In the incoming states they simply coincide with the usual Fermi distribution functions for a given temperature and voltages applied, and, therefore, they depend only on the energies ε but not on the angles θ and ϕ . Using the particle conservation law the distribution functions of the outgoing states can be rewritten as

$$f_{\alpha}^{out}(\varepsilon, \theta) = \sum_{\beta, n} \int d\phi |t_{\beta\alpha}(\varepsilon + n\hbar\Omega, \phi; \varepsilon, \theta)|^2 f_{\beta}^{in}(\varepsilon + n\hbar\Omega). \quad (2.3)$$

The total current flowing through the strip takes the form

$$I = 4W \int \frac{p dp d\theta}{(2\pi\hbar)^2} ev \cos \theta (f_L^{in}(\varepsilon(p)) - f_L^{out}(\varepsilon(p), \theta)) \quad (2.4)$$

where W is the junction width, and v is the velocity of electrons. The coefficient 4 in the last equation accounts for the spin and valley degeneracies of the quasiparticle spectrum in graphene. Using Eqs. (2.2) and (2.3), we rewrite Eq. (2.4) as

$$I = 4W \int \frac{p dp d\theta}{(2\pi\hbar)^2} ev \cos \theta \sum_{\beta, n} \int d\phi \times \\ \times (|t_{L\beta}(\varepsilon, \theta; \varepsilon + n\hbar\Omega, \phi)|^2 f_L^{in}(\varepsilon) - \\ - |t_{\beta L}(\varepsilon + n\hbar\Omega, \phi; \varepsilon, \theta)|^2 f_{\beta}^{in}(\varepsilon + n\hbar\Omega)). \quad (2.5)$$

Changing the variables in Eq. (2.5) and using the transverse momentum conservation law, $p^{in}(\varepsilon^{in}) \sin \theta^{in} = p^{out}(\varepsilon^{out}) \sin \theta^{out}$, one can see that the terms with $\beta = L$ vanish. Indeed, they are responsible for the backscattering and therefore cannot contribute to the current through the junction.

If the time-periodic EF possesses the time-reversal symmetry ($t \rightarrow -t$), with respect to some moment of time $t = 0$, e.g. if the EF is sinusoidal, then the relation

$$|t_{LR}(\varepsilon, \theta, \varepsilon + n\hbar\Omega, \phi)|^2 = |t_{RL}(\varepsilon + n\hbar\Omega, \phi; \varepsilon, \theta)|^2 \quad (2.6)$$

holds, and Eq. (2.5) can be reduced to

$$I = 4W \int \frac{p dp d\theta}{(2\pi\hbar)^2} ev \cos \theta \times \\ \times \sum_n P_{LR}(\varepsilon, \varepsilon + n\hbar\Omega, \theta) (f_L^{in}(\varepsilon) - f_R^{in}(\varepsilon + n\hbar\Omega)), \quad (2.7)$$

where the function

$$P_{LR}(\varepsilon, \varepsilon + n\hbar\Omega, \theta) = \int d\phi |t_{LR}(\varepsilon, \theta, \varepsilon + n\hbar\Omega, \phi)|^2, \quad (2.8)$$

is the probability for a particle in the state $|\varepsilon, \theta\rangle_L^{in}$ in the left lead to be scattered into the right lead into the state with the energy $\varepsilon + n\hbar\Omega$.

This is the most general expression for the current that can be derived using only the symmetries of the Hamiltonian of the system and the particle conservation law. The total current I contains the elastic component (the term with $n = 0$) and inelastic components corresponding to the terms with $n \neq 0$. Let us emphasize that the radiation not only induces the current due to the inelastic processes but also leads to the modification of the probability $P_{LR}(\varepsilon, \varepsilon, \theta)$ of the elastic scattering. In the next sections we show that this probability can be strongly suppressed by the external radiation, which results in the vanishing of the current through the graphene strip. Moreover, in systems where the inelastic scattering violates symmetries in such a way that

$$P_{LR}(\varepsilon, \varepsilon + n\hbar\Omega, \theta) \neq P_{LR}(\varepsilon + n\hbar\Omega, \varepsilon, \theta), \quad (2.9)$$

the external radiation generates a photocurrent, i.e. the directed current without any external voltage applied to the junction³⁷.

In a related paper, Ref. 36, the possibility of the photocurrent has been overlooked since there was not considered inelastic transmission of electrons through the junction, corresponding to the terms with $n \neq 0$ in Eq. (2.7).

The probabilities $P_{LR}(\varepsilon, \varepsilon + n\hbar\Omega, \theta)$ can be calculated explicitly as soon as the Hamiltonian of the system under consideration is given. In the next two sections we find the probabilities $P_{LR}(\varepsilon, \varepsilon + n\hbar\Omega, \theta)$ for the quantum mechanical problem of electron motion in graphene in an external potential $U(\mathbf{r})$ and irradiated by a time-periodic EF.

III. EF-INDUCED DYNAMICAL GAPS AND ELECTRON DYNAMICAL TUNNELING

To elucidate the main phenomena related to the influence of radiation on the transport in graphene, we first consider the modification of the quasiparticle spectra due to the presence of a monochromatic electromagnetic wave, and their tunneling through smooth potential barriers. For simplicity, we neglect in the next two sections scattering due to impurities and electron-phonon interaction.

The states of electrons in graphene are conveniently described by the four-component wavefunctions, defined on two sublattices and two valleys. Since we consider the transport in an infinite clean sample, we may neglect intervalley- and spin scattering and study the propagation of electrons for different valleys and spin directions separately.

Electron motion in the time-dependent EF is described by the non-stationary Schrödinger equation,

$$i\hbar \frac{\partial \psi}{\partial t} = \hat{H} \psi, \quad (3.1)$$

where \hat{H} is the full Hamiltonian of the system.

Near the point where the bands of graphene touch each other (Dirac point) a simplified Hamiltonian $\hat{\mathcal{H}}$ of a low-energy quasiparticle moving in a slowly varying static potential $U(\mathbf{r})$ and interacting with an external electromagnetic radiation can be written for a single valley and for a certain direction of spin as³⁸

$$\hat{\mathcal{H}} = v\hat{\sigma} \left(\mathbf{p} - \frac{e}{c} \mathbf{A}(t) \right) + U(\mathbf{r}). \quad (3.2)$$

Here \mathbf{p} is the momentum of the quasiparticle, v – the Fermi velocity, and $\hat{\sigma}$ – the vector of the Pauli matrices in the sublattice space ("pseudospin" space).

The electromagnetic radiation is taken into account choosing a proper vector potential $\mathbf{A}(t)$. For a linearly polarized monochromatic electromagnetic wave it can be taken in the form

$$\mathbf{A}(t) = \frac{c}{\Omega} \mathbf{E} \cos(\Omega t), \quad (3.3)$$

where \mathbf{E} is the amplitude of the electric field in the wave.

Substituting Eq. (3.2) into Eq. (3.3) and using Eq. (3.1) we obtain a complete description of electron motion of graphene. In the next three subsections we study the properties of solutions of the time-dependent Schrödinger equation in graphene in presence of linearly polarized monochromatic radiation.

A. Dynamical gap in the quasiparticle spectra

As it has been shown long ago, in the Ref. 27, resonant interaction of quasiparticles with EF can lead to the formation of a dynamical gap in the electron spectrum of semiconductor. The dynamical gap occurs in the vicinity of the values of momentum \mathbf{p} , determined by the resonant condition $\epsilon_c(\mathbf{p}) - \epsilon_v(\mathbf{p}) = \hbar\Omega$, where $\epsilon_v(\mathbf{p})$ and $\epsilon_c(\mathbf{p})$ are the electron energies in the valence and conduction bands respectively.

In order to illustrate this, let us consider an electron propagating in the absence of external potential potential [$U(\mathbf{r}) = 0$] along a certain z axis with momentum \mathbf{p} , perpendicular to the field \mathbf{E} , which is assumed to be directed along the x axis in the plane of the graphene sheet (Fig. 1).

Let us emphasize, that our choice of the coordinate system and associated pseudospin basis differs from that usually chosen in graphene-related papers. Usually, all the calculations are done in the basis of states, defined on different graphene sublattices, so that the z axis is directed perpendicularly to the graphene plane, while x and y belong to the plane. However, for the purposes of the present paper it is more convenient to work with the

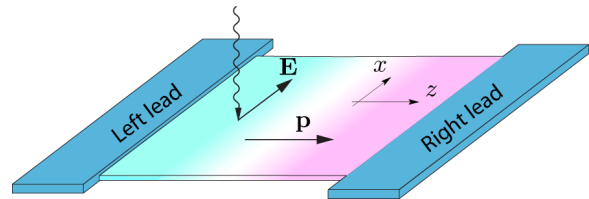


FIG. 1: (Color online) Graphene junction in presence of external radiation. Axis z is directed along the electron momentum \mathbf{p} in the graphene plane, axis x - parallel to the electric field \mathbf{E} in the external electromagnetic wave.

Hamiltonian, having a diagonal form in the basis of states {"pseudospin parallel to the momentum \mathbf{p} ", "pseudospin antiparallel to \mathbf{p} " }.

For this choice of the coordinate system the Hamiltonian [Eq. (3.2)] takes the form

$$\hat{\mathcal{H}} = vp_z \hat{\sigma}_z + 2\Delta \hat{\sigma}_x \cos(\Omega t), \quad (3.4)$$

where

$$\Delta = \frac{v|e|E}{2\Omega}. \quad (3.5)$$

As it will be clear from the analysis below, even a weak EF ($\Delta \ll \hbar\Omega$) strongly affects the motion of electrons with momenta close to the resonant values,

$$p_{res} = \pm \frac{\hbar\Omega}{2v}, \quad (3.6)$$

which makes this region of momenta the most interesting. Therefore, we consider now a quasiparticle with momentum p_z close to one of these resonant values, say, to $\hbar\Omega/(2v)$. Applying the rotating-wave approximation (RWA)³⁹, we decompose the second term of the Hamiltonian (3.4) into the right and the left circularly-polarized waves, rotating about z axis in the pseudospin space, and neglect the second one in the vicinity of the resonance chosen. In the other words, we make the following replacement in Eq. (3.4):

$$2\Delta \hat{\sigma}_x \cos(\Omega t) \longrightarrow \Delta (\hat{\sigma}_x \cos(\Omega t) + \hat{\sigma}_y \sin(\Omega t)). \quad (3.7)$$

Then, going to the reference frame (RF) rotating counterclockwise about the z axis with the angular velocity Ω in the pseudospin space, we come to a problem with a static Hamiltonian. This procedure corresponds to the application of the unitary transformation

$$\hat{U} = e^{i\frac{\Omega t}{2} \hat{\sigma}_z} \quad (3.8)$$

to the two-component wavefunctions. In the new basis we obtain the time-independent effective Hamiltonian

$$\hat{\mathcal{H}}' = \left(vp_z - \frac{\hbar\Omega}{2} \right) \hat{\sigma}_z + \Delta \hat{\sigma}_x. \quad (3.9)$$

The eigenvalues of the Hamiltonian (3.9) determine the quasiparticle spectrum as

$$\varepsilon_{e,h}(p_z) = \pm \left[\left(vp_z - \frac{\hbar\Omega}{2} \right)^2 + \Delta^2 \right]^{\frac{1}{2}}. \quad (3.10)$$

Equation (3.10) shows that the spectrum acquires a dynamical gap 2Δ at the resonant value of momentum. This gap is proportional to the amplitude E of the radiation and inversely proportional to its frequency Ω . Far from the resonance ($|p_z v - \hbar\Omega/2| \gg \Delta$), the corresponding quasiparticles are just conventional electrons and holes in the absence of radiation, having spectra $\pm|vp_z - \hbar\Omega/2|$ in the chosen rotating RF.

When the momentum p_z approaches the other resonance, $-\hbar\Omega/2v$, one can analogously calculate the quasiparticles spectra in the RWA in the RF rotating clockwise about the z axis,

$$\varepsilon_{e,h}(p_z) = \pm \left[\left(vp_z + \frac{\hbar\Omega}{2} \right)^2 + \Delta^2 \right]^{\frac{1}{2}}. \quad (3.11)$$

Let us emphasize that the applicability of the RWA for the derivation of each of the Eqs. (3.10) and (3.11) is limited not by the closeness of the momentum to the corresponding resonance, but by the negligibility of the influence of the other resonance. For instance, Eq. (3.10) is valid as soon as

$$\left| p_z + \frac{\hbar\Omega}{2v} \right| \gg \frac{\Delta}{v}. \quad (3.12)$$

The dynamical gaps in the quasiparticle spectra have been calculated assuming that EF was linearly polarized perpendicular to the direction of momentum \mathbf{p} . If the field \mathbf{E} is directed at some angle γ with respect to its transverse component \mathbf{E}_\perp , perpendicular to \mathbf{p} , then the effective dynamical gap decreases and becomes equal to

$$\tilde{\Delta}(\gamma) = \Delta \cos \gamma. \quad (3.13)$$

As we will show in Sec. VII, for the reasonable values of the radiation power this gap is much smaller than all the other energy scales in the problem, such as the Fermi energy, the photon energy $\hbar\Omega$, the heights of the potential barriers, and the typical voltages applied to a sample.

Radiation-induced gaps have been observed in the spectra of spontaneous radiation of conventional semiconductors subject to a strong monochromatic laser field^{31,32}. In this paper we consider the effect of radiation on the *transport* properties of graphene. Measurement of the current is a simpler task and we hope that the corresponding experiments are also possible.

In the limit of small value of Δ considered here ($\Delta \ll \hbar\Omega$), the conductivity of a homogeneous irradiated semiconductor sample³³ or the conductance of a tunnel junction between two irradiated uniform samples²⁷ can be strongly affected by the radiation only provided the

Fermi level is close to the position of the EF-induced gap. Any considerable spatial variation of potential due to inhomogeneities in the system smears the gap and makes its observation in bulk semiconductors very difficult.

In the present paper we consider an essentially different situation when electrons move in a non-uniform step-like potential and their chemical potentials in the left and the right reservoirs are not necessarily close to those, corresponding to the resonant momenta. Nevertheless, for a broad interval of energies of the incident electrons each of them achieves resonances in one or several *resonant points*.

The reason for this unusual behavior is the coordinate dependence of the electron momenta that determine the behavior of the wavefunctions. The momenta of electrons reach their resonant values near the step. The region, where these momenta correspond to the motion inside the dynamical gap, is thus localized in space close to the step-like potential. Electrons must tunnel through the gap in order to contribute to the current between the leads. In the regions between the resonant points electrons weakly interact with the radiation and propagate freely. However, the current-voltage characteristic of such a junction is determined by the tunneling through the dynamical gaps.

B. Dynamics of electrons normally incident on irradiated potential barrier

In this and the next subsections we study the tunneling through the dynamical gap in the momentum space in the vicinity of the resonant point.

Consider first an electron *normally* incident on a smooth potential barrier $U(\mathbf{r}) = U(z)$, varying only in one dimension. To be specific, we assume that the electron is moving in the conduction band along the z axis, and the height of the potential barrier increases with z . Let ε be the total electron energy (kinetic+potential) in the initial laboratory RF far from the resonant point z_0 [determined by the equation $U(z_0) = \varepsilon - \frac{\hbar\Omega}{2}$], where the momentum in the absence of the radiation would equal to the resonant value $\hbar\Omega/2v$ (see Fig. 2). The EF in the graphene plane is polarized perpendicularly to the z axis, the direction of electron momentum.

As follows from the Hamiltonian (3.2), the electron velocity far from the resonance, where $|U(z) - U(z_0)| \gg \Delta$, is determined by its pseudospin:

$$\mathbf{v} = v\hat{\sigma}. \quad (3.14)$$

This means that far from the resonant point the velocities and the pseudospin $|\uparrow\rangle$ of the incident $e^{i\hbar^{-1}\int^z p(z)dz}$ and the transmitted $te^{i\hbar^{-1}\int^z p(z)dz}$ waves are both directed along the z -axis. The momentum $p(z)$ entering the exponents is determined by the equation

$$p(z) = (\varepsilon - U(z))/v. \quad (3.15)$$

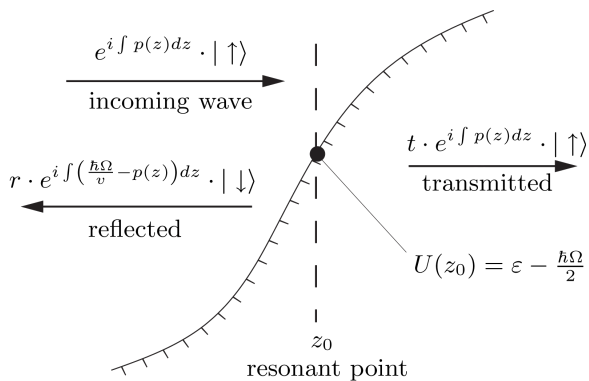


FIG. 2: Scattering of quasiparticles moving perpendicularly to the barrier.

Let us emphasize, that in contrast to the corresponding quasiclassical expression for the Schrödinger equation, Eq. (3.15) is exact, i.e. valid for arbitrary values of momenta \mathbf{p} , which follows immediately from the Dirac-type Hamiltonian (3.2). According to our notations, the pseudospin $|\downarrow\rangle$ of the reflected wave is antiparallel to the z axis.

Let us find the transmission and reflection coefficients of the electron in the region of the barrier where it strongly interacts with the radiation. In the pseudospin space we go to the rotating RF defined by transformation (3.8). In this frame the Hamiltonian is static, the particle has energy $\varepsilon - \frac{\hbar\Omega}{2}$ and scatters elastically. The transmission and reflection coefficients are found solving the Dirac equation for the quasiparticle wavefunctions close to the resonant point. In the presence of the potential $U(z)$ this equation takes the form

$$\left[\left(v\hat{p}_z - \frac{\hbar\Omega}{2} \right) \hat{\sigma}_z + \Delta\hat{\sigma}_x + U(z) \right] \Psi = \varepsilon\Psi. \quad (3.16)$$

Here Ψ is the two-component wavefunction.

Without losing generality, we can set $z_0 = 0$. Since the potential is smooth, it can be expanded in small z and become linear around the resonant point:

$$U(z) \approx \varepsilon - \frac{\hbar\Omega}{2} + Fz. \quad (3.17)$$

The Dirac equation for the particle with energy $\varepsilon - \frac{\hbar\Omega}{2}$ can be written in the momentum representation as

$$-i\hbar F \frac{\partial}{\partial p} \Psi(p) = \left(\hat{\sigma}_z v \left(p - \frac{\hbar\Omega}{2v} \right) + \Delta\hat{\sigma}_x \right) \Psi(p) \quad (3.18)$$

We have taken into account that in the momentum representation $\hat{z} = i\hbar \frac{\partial}{\partial p}$.

Equation (3.18) describes Landau-Zener tunneling through the dynamical gap (Fig. 3) in the momentum space. This phenomenon is analogous to the electron tunneling through the forbidden band in a conventional semiconductor tunnel p-n junctions⁴⁰ or through a non-irradiated graphene p-n junctions, when the incident electron has some finite transverse component of momentum.

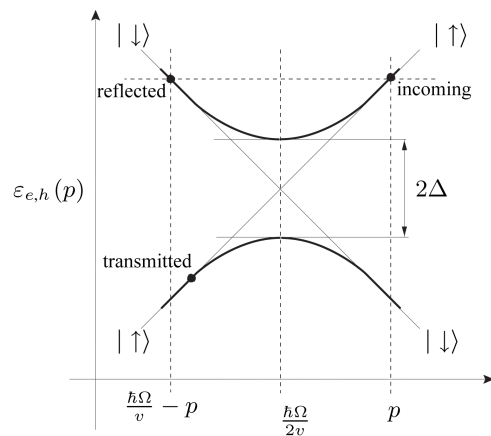


FIG. 3: Tunneling through the dynamical gap in the momentum space (rotating RF). The quasiparticle spectrum in presence of radiation, Eq. (3.10), is shown by the solid lines in the plot, the spectrum in absence of radiation - by the thin lines.

The latter case, when the role of the gap is played by the quasiparticle energy at zero longitudinal momentum, has been studied in the Refs. 41 and 42.

Equation (3.18) can be solved exactly and the tunneling probability $T = |t|^2$ takes the form

$$T = e^{-\frac{\pi\Delta^2}{\hbar v F}}. \quad (3.19)$$

We emphasize that Eq. (3.19) gives the exact probability of Landau-Zener tunneling, i.e. it is valid for arbitrary values of the parameter

$$\mathcal{L} = \frac{\pi\Delta^2}{\hbar v F} \quad (3.20)$$

in the exponent rather than only in the “quasiclassical” limit ($\mathcal{L} \gg 1$), considered in the previous papers^{36,43}.

According to the energy conservation law in the rotating RF, the reflected wave has the momentum $\frac{\hbar\Omega}{v} - p(z)$ at the same point z , where the incident wave had momentum $p(z)$ (Fig. 3). This momentum corresponds to the energy $\varepsilon - \hbar\Omega$ of the scattered electron in the initial laboratory RF. This means, that reflecting from the resonant point the electron emits a photon of the energy $\hbar\Omega$.

Similarly, one can consider the cases of the quasiparticle scattering in the valence band of graphene at the resonant points, where the momentum in absence of radiation equals the other resonant value $-\frac{\hbar\Omega}{2v}$.

So, we conclude that an electron normally incident on an irradiated potential barrier can pass with the probability T through the resonant point, where its kinetic energy vp in absence of radiation would be equal $\hbar\Omega/2$ or be reflected from that point with the probability $1 - T$, emitting a photon of energy $\hbar\Omega$. At the other type of the resonant points, where the kinetic energy in the absence of radiation equals $-\hbar\Omega/2$, the particle absorbs a

photon of energy $\hbar\Omega$ during the reflection. The emission/absorption is accompanied by the particle reflection and the pseudospin-flip.

Tunneling suppression. Applying strong radiation or smooth potential barriers, such that $\mathcal{L} \gg 1$, one can achieve small tunneling probabilities $T \ll 1$ [Eq. (3.19)]. Such a situation was considered in the Ref. 36, where it was argued that in this case one would be able to suppress Klein tunneling and confine electrons by irradiated barriers. In Sec. VII we revisit this issue and estimate the radiation power needed to realize such a confinement.

Limit of small \mathcal{L} . Let us show now, that in presence of impurities, electron-phonon and electron-electron interactions in the sample in the limit $\mathcal{L} \ll 1$ the probabilities of reflection and transmission at the resonant point remain the same as in the ballistic sample even for the radiation intensities S much below the critical value S_c , at which the gap is suppressed in a wide uniform sample. Making this statement we imply that \mathcal{L} is given in Eq. (3.20) with Δ being not the real dynamical gap, but the quantity defined by Eq. (3.5), which gives the value of the gap for a clean sample neglecting impurities, electron-phonon and electron-electron interactions.

For small \mathcal{L} Landau-Zener tunneling in the ballistic sample occurs in the momentum interval of the order of

$$\Delta p_{LZ} \sim \sqrt{\frac{\hbar F}{v}}. \quad (3.21)$$

In the coordinate space the corresponding tunneling length is

$$\Delta r_{LZ} = \frac{v \Delta p_{LZ}}{F} \sim \sqrt{\frac{\hbar v}{F}}. \quad (3.22)$$

Note, that the scales (3.21) and (3.22) are determined by the potential slope only and do not depend on the value of the gap.

Equation (3.22) shows that the perturbation $\Delta\hat{\sigma}_x$ in the quasiparticles Hamiltonian (3.4) induces transitions between the states $|\uparrow\rangle$ and $|\downarrow\rangle$ in a wide spatial interval independent of Δ . This occurs even when the dynamical gap in the particle spectrum is smeared due to the radiation-independent relaxation processes.

The effect of the radiation-independent relaxation on the Landau-Zener tunneling can be neglected provided the probability of excitation due to it is much smaller than 1, or, in other words, the relaxation time τ_R is sufficiently large

$$\tau_R \gg \sqrt{\frac{\hbar}{vF}}. \quad (3.23)$$

This condition does not necessarily imply that the probability of reflection $\mathcal{L} = \pi\Delta^2/(\hbar vF)$ in the Landau-Zener tunneling is much larger than the probability of an EF-independent transition on the corresponding interval. However, using the inequality (3.23) will allow us to consider the EF-independent transitions and the tunneling independently of each other in the calculation of the photocurrent in the subsequent sections.

C. Radiation-induced hops between trajectories at the resonant points

In the previous subsection we considered electrons incident normally on a potential barrier in a transverse EF. In this subsection we analyze the scattering in the presence of radiation for arbitrary angles between the electron momentum \mathbf{p} at the resonant point, the slope of the potential $dU/d\mathbf{r}$, and the field \mathbf{E} .

As it has been already mentioned [cf. Eq. (3.13)], the effective dynamical gap close to the resonant point is $\tilde{\Delta} = \Delta \cos \gamma$, where

$$\gamma = \frac{\pi}{2} - (\widehat{\mathbf{p}}, \widehat{\mathbf{E}}) \quad (3.24)$$

is the angle between the field \mathbf{E} and its transverse component \mathbf{E}_\perp , perpendicular to the momentum \mathbf{p} .

The effective potential slope along the direction of the electron momentum at the resonant point is $\tilde{F} = |F \cos \beta|$, where

$$\beta = (\widehat{dU/d\mathbf{r}}, \widehat{\mathbf{p}}) \quad (3.25)$$

is the angle between the slope of the potential and the momentum at the resonant point.

Then, instead of Eq. (3.19), one should use the formula

$$T = e^{-\frac{\pi\Delta^2 \cos^2 \gamma}{\hbar v |F \cos \beta|}} \quad (3.26)$$

for the probability for an electron to pass through the resonant area without being scattered by the radiation. Below we will present an explicit derivation of this result.

Note also that, although being reflected at the resonant point the electron changes its pseudospin (direction of velocity), it does not necessarily follow the same trajectory along which it moved towards the resonant point. The reason is that the reflection is accompanied by a photon emission or absorption, and the new electron energy $\varepsilon_{refl} = \varepsilon \pm \hbar\Omega$ corresponds to a new trajectory. This means that the radiation can enforce the electron to hop onto the trajectory, corresponding to the opposite pseudospin at the resonant point (Fig. 4). Let us now proceed to an explicit derivation of this result and of Eq. (3.26).

As discussed in the previous subsection, far from the resonances the electron motion can be considered quasiclassically neglecting the radiation. Let AOB (Fig. 4) be a classical trajectory of a quasiparticle moving in absence of radiation in the potential $U(\mathbf{r})$. Here, O is the resonant point where the momentum equals the resonant value $p = \hbar\Omega/(2v)$. At the resonant point the particle can be reflected and hop to the other trajectory COD . Trajectory COD corresponds to the same momentum but the *opposite* pseudospin at the resonant point (Fig. 4).

To obtain the Eq. (3.26) and analyze the radiation-induced hops between trajectories we introduce at each point of AOB the coordinate system $\eta\zeta\xi$, where the axis ξ is directed tangentially along the trajectory, ζ - normally to the graphene sheet, and η lies in the plane of

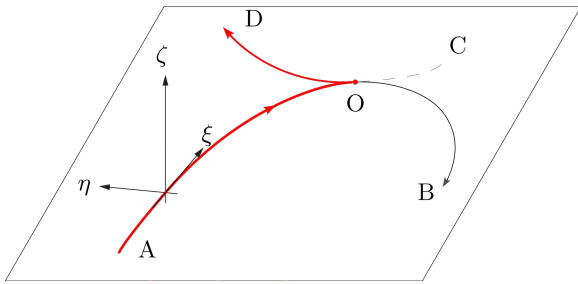


FIG. 4: (Color online) Radiation-induced hop to the trajectory with opposite pseudospin at the resonant point. Moving initially along the arc AO, at the resonant point O the quasi-particle either hops to the trajectory OD, if scattered by the radiation, or continues moving along OB, in case the scattering has not occurred. Axis ξ of the coordinate system is directed along the trajectory AOB at each point, axis ζ is perpendicular to the graphene plane, and η lies in the plane.

the sheet. Let s be the particle coordinate along the trajectory AOB . Introduce also the fixed coordinate system xyz , such that the x axis is directed along the EF and y -normally to the graphene plane and along ζ . The system $\eta\xi\xi$ is obtained rotating xyz -system around the y axis by some angle $\alpha(s)$.

The corresponding pseudospin transformation is

$$\hat{W} = e^{\frac{i}{2}\alpha(s)(\mathbf{e}_\zeta \hat{\sigma})}. \quad (3.27)$$

Let us set $s = 0$ at the resonant point. The Hamiltonian (3.2), written in the pseudospin basis defined by the system $\eta\xi\xi$ and linearized in the vicinity of the point O, takes the form

$$\begin{aligned} \hat{H} &= i\hat{W}\hat{W}^\dagger + \hat{W}\hat{\mathcal{H}}\hat{W}^\dagger \\ &= \hat{\sigma}_z v \left(p_\xi - \hbar \frac{\partial \alpha}{\partial s} \hat{\sigma}_y \right) + \frac{\partial U}{\partial s} s \\ &\quad + \hat{\sigma}_x v p_\eta + \frac{\partial U}{\partial \eta} \eta \\ &+ 2\Delta(\hat{\sigma}_z \sin \alpha + \hat{\sigma}_x \cos \alpha) \cos(\Omega t). \end{aligned} \quad (3.28)$$

The third line of Eq. (3.28) describes the motion of the wavepacket in the direction of axis η , perpendicular to the trajectory. This part of the Hamiltonian is independent of the longitudinal coordinates on the scales being considered and can be disregarded if we want to find the probability of tunneling through the point O along the trajectory AOB.

The term $-\hbar(\partial\alpha/\partial s)\hat{\sigma}_y$ in the second line of Eq. (3.28) is the gauge potential generated by the local rotations of the reference frame $\eta\xi\xi$. Considering the tunneling in the vicinity of the point O, one can neglect this term, provided that the potential is smooth enough ($\lambda/v \gg \Omega$, where λ is the characteristic scale of the potential variation). Note, that such a neglect in general can be made only on a small enough interval, but not on the whole trajectory between different resonant points.

In the related paper, Ref. 36, the local reference frame reverted the direction of two axes at the point where $p =$

0, but the corresponding non-negligible delta-function-type gauge potential, generated by this rotation, was not taken into account.

The last line of Eq. (3.28) is the EF-induced time-dependent perturbation of the Hamiltonian. Following the same line of reasoning as when deriving RWA³⁹, one can keep in this perturbation only the transverse circularly polarized wave rotating clockwise about \mathbf{p} (axis ξ).

Making all the aforementioned approximations in the Eq. (3.28) and going to the rotating RF, we arrive at the same problem as considered in the previous subsection with the effective gap $\Delta \cos \gamma$ and the effective potential slope $F \cos \beta$, and finally obtain the Eq. (3.26).

IV. DYNAMICS OF ELECTRONS IN A BALLISTIC GRAPHENE P-N JUNCTION

From now on we restrict ourselves to the consideration of a specific type of potential barriers. We assume that the potential $U(z)$, varying only along a certain axis z , increases monotonically from $U(-\infty) = 0$ far in the left lead to $U(+\infty) = U_0 > 0$ far in the right one. The electric field \mathbf{E} of the external radiation is directed along the x axis, perpendicular to the z axis and lying in the graphene plain.

From the previous section we know that the electron motion in a non-uniform potential in the presence of radiation can be considered as quasiclassical between the resonant points, where the hops between trajectories can take place, accompanied by the pseudospin-flips and photon emissions or absorptions.

Now we have to consider all the classical electron trajectories in the potential under consideration and find their resonant points.

A. Dynamics of electrons non-interacting with radiation

In the absence of radiation electron transmission through the junction is determined by its transverse momentum $p_\perp = p \sin \theta$, which is conserved during the motion. The electron tunnels through the non-irradiated p-n junction with the probability⁴¹

$$T_0 = e^{-\frac{\pi p_\perp^2 v}{\hbar F_0}}, \quad (4.1)$$

and, accordingly, reflects back with the probability $1 - T_0$. Here F_0 is the effective potential slope at the p-n interface, calculated taking into account the charge density distribution in the junction⁴⁴. For each incident electron F_0 should be understood as the slope of the potential at the point where the longitudinal momentum equals zero. Note, that in general it is different from the potential slope F at the resonant point.

Let us classify the regimes of the particle motion in the absence of radiation according to their transverse momenta. We introduce the “2D-modes”, with

$|p_{\perp}| \gg (\hbar F_0/(\pi v))^{\frac{1}{2}}$, and the “normal modes”, with $|p_{\perp}| \ll (\hbar F_0/(\pi v))^{\frac{1}{2}}$. In the first case, for large enough p_{\perp} , the electrons perfectly reflect from the interface, from the place where their longitudinal momentum turns to zero. In the second case particles freely penetrate through the junction without reflection.

The classical path of an electron in the presence of the radiation consists of the pieces of its paths in the absence of the radiation, stuck to each other at the resonant points.

Let us show now that on each electron trajectory in the presence of the radiation there can be *no more than two resonant points*. An electron encounters a resonant point, when its full momentum $(p_z^2 + p_{\perp}^2)^{\frac{1}{2}}$ reaches the resonant value $\hbar\Omega/(2v)$, i.e. when the longitudinal momentum p_z becomes equal to one of the two values

$$p_{res} = \pm \left[\left(\frac{\hbar\Omega}{2v} \right)^2 - p_{\perp}^2 \right]^{\frac{1}{2}}. \quad (4.2)$$

The momentum p_z of a classical electron, moving in the monotonically increasing potential $U(z)$, changes in time monotonically, $\dot{p}_z = -\partial_z U < 0$. If the particle scatters at a resonant point, its momentum does not change. Then each of the momentum values (4.2) of p_z is reached not more than once, and the electron encounters correspondingly not more than two resonant points.

In order to calculate the total current through the junction we have to consider the electron paths starting from the left lead and terminating in the right lead. The contribution to the current of the inverted processes, transmission from right to left, has been already taken into account during the derivation of Eq. (2.7).

B. Electron paths in effectively two-dimensional modes.

Let us find first the resonant points for an electron in the “2D-mode”, i.e. having large $|p_{\perp}|$, and incident on the barrier from the left with a positive energy and momentum $p > \hbar\Omega/(2v)$.

If $|p_{\perp}| > \hbar\Omega/(2v)$, then there are no resonant points on the trajectory. The electron weakly interacts with EF, perfectly rebounds from the p-n interface in presence of radiation and thus does not contribute to the current through the junction.

If $|p_{\perp}| < \hbar\Omega/(2v)$ and the potential U_0 is high enough, then there are two resonant points, corresponding to the values (4.2) of momentum p_z .

The behavior of the particle is best illustrated as its path on the plot of its kinetic energy in the laboratory RF,

$$\varepsilon_{kin}(p_z) = \pm v(p_{\perp}^2 + p_z^2)^{\frac{1}{2}}, \quad (4.3)$$

versus the longitudinal momentum p_z .

Consider, for instance, the process illustrated in the Fig. 5(a). Spectrum (4.3) is shown by the dashed lines there. The electron path on this plot, indicated by solid lines with arrows, starts at the branch of the spectrum corresponding to the conduction band and positive velocity $v_z = \partial\varepsilon/\partial p_z$. If there was no radiation, the electron would always be in the conduction band and would follow the dotted line in the figure. In the end of the dotted line $v_z < 0$, indicating the fact that the electron would have reflected from the junction. In fact, when reaching the first resonant point, in the process under consideration the electron emits a photon [curved line in the Fig. 5(a)], and then moves in the valence band, passing through the second resonant point. In the end of the process the sign of the longitudinal velocity coincides with the initial one. This means, that as a result of the process, the electron penetrated through the junction from one lead into another. Thus, the radiation can assist electron transmission through the junction.

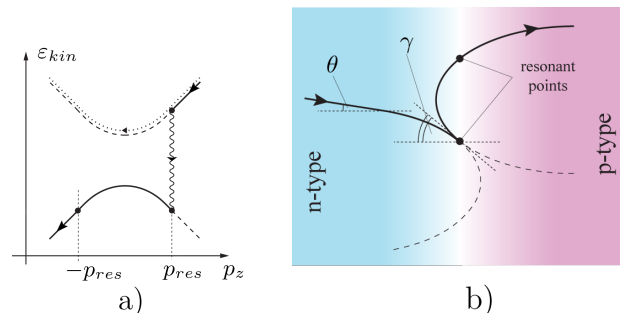


FIG. 5: (Color online) Process contributing to the current through the junction (solid lines). The particle emits a photon at the first resonant point, and passes without reflection the second (“2D-modes”). (a) In the plot “kinetic energy vs. longitudinal momentum”. (b) In the spatial coordinate space (graphene plane view). The emission of the photon is accompanied by the hop at the resonant point between two classical paths, obtained in absence of radiation.

Let us now take a look at the corresponding electron trajectory in the coordinate space, Fig. 5(b). Shown there two classical trajectories in absence of radiation are tangent at the resonant point. The left trajectory in the absence of radiation starts and ends up in the region of n-type graphene. It is the path of the electron in the conduction band, having classical Hamiltonian

$$\hat{\mathcal{H}}_{cond}(\mathbf{p}, \mathbf{r}) = vp + U(\mathbf{r}). \quad (4.4)$$

Similarly, the right path begins and terminates in the p-type graphene, and corresponds to the motion of a particle in the valence band with the Hamiltonian

$$\hat{\mathcal{H}}_{val}(\mathbf{p}, \mathbf{r}) = -vp + U(\mathbf{r}). \quad (4.5)$$

Due to the effect of the radiation the particle hops at the resonant point from the left path to the right one, the whole resulting trajectory is shown by the solid line in the Fig. 5(b).

For a given electron energy and the angle of incidence the probability to pass along the trajectory under consideration is

$$P_{1scatt,2pass} = (1 - T_1)T_2, \quad (4.6)$$

where T_1 and T_2 are the transmission probabilities correspondingly at the first and the second resonant points.

Analogous to Fig. 5, Fig. 6 illustrates the tunneling, when the particle is not scattered at the first resonant point, but rebounds from the second one, emitting a photon.

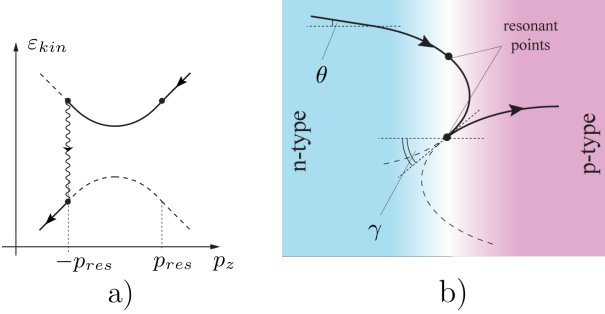


FIG. 6: (Color online) Another process contributing to the current through the junction (solid lines). The particle passes without reflection the first resonant point and emits a photon at the second (“2D-modes”). (a) In the plot “kinetic energy vs. longitudinal momentum”. (b) In the spatial coordinate space (graphene plane view). The emission of the photon is accompanied by the hop at the resonant point between two classical paths, obtained in absence of radiation.

Let us emphasize, that one should not confound the static gap $2v|p_\perp|$ of the Hamiltonian

$$\hat{\mathcal{H}}_{kin}(p_z) = vp_z\hat{\sigma}_z + vp_\perp\hat{\sigma}_x, \quad (4.7)$$

giving the particle spectrum in the absence of radiation in the Figs. 5 and 6, with the dynamical gap 2Δ in Fig. 3, where the quasiparticles spectrum is shown in the rotating reference frame, taking into account the radiation. Landau-Zener tunneling through the static gap is strongly suppressed, since $|p_\perp| \gg (\hbar F_0/(\pi v))^{1/2}$.

In the processes shown in the plots in Figs. 5(a) and 6(a), electron ends up in the right lead, because finally the particle is on the branch of the spectrum corresponding to the same direction of velocity at $|p_z| \rightarrow \infty$ as on the initial one. In contrast to that, Fig. 7 illustrates the backscattering: the particles enter and leave the junction in the same lead L. According to the results of Sec. II, the corresponding trajectories do not contribute to the current and should be excluded from our consideration.

We see that, although in the absence of radiation electrons in the normal modes could not tunnel through the junction, they can penetrate from the left to the right lead emitting one photon when the sample is irradiated by EF. Due to the time-reversal symmetry, the inverse processes, when a particle penetrates from the right to

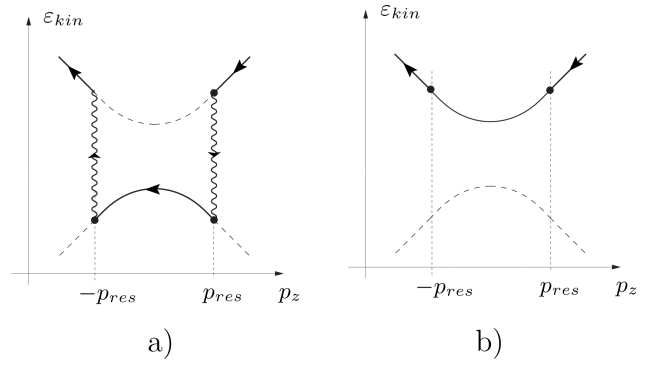


FIG. 7: Kinetic energies of the particles incident from the left reservoir and scattered back there (“2D-modes”). a) The particle emits and absorbs a photon at the first and the second resonant points correspondingly. b) The particle is not scattered by the radiation.

the left lead absorbing a photon, also exist. As we discussed before, in order to derive the current-voltage characteristics of the junction, we have to calculate the tunneling probabilities only for the particles incident from the left, the contribution of inversed processes has been taken into account when deriving Eq. (2.7).

C. Electron paths in normal modes.

Now let us consider the normal modes, i.e. having such small transverse momenta that in the momentum space the particles freely penetrate through the static gap, as if it was zero. This corresponds to $p_\perp = 0$ in Eq. (4.3).

For the tunneling from the left to the right lead both possible electron paths $\varepsilon_{kin}(p_z)$ are shown in Fig. 8.

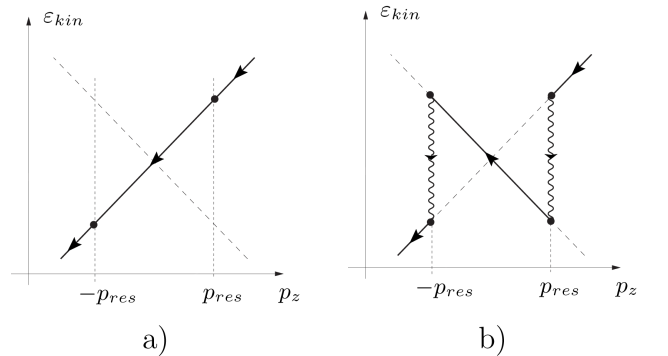


FIG. 8: Kinetic energies of the particles incident from the left reservoir and penetrating into the right one (normal modes). a) Usual Klein tunneling, no radiation-induced scattering. b) Tunneling accompanied by the two-photon emission.

The first one, in the Fig. 8(a), corresponds to the usual Klein tunneling, when the particle is not scattered by the radiation. The static gap is negligible, so the particle

passes from the conduction to the valence band through the Dirac point without reflection.

The second path, in the Fig. 8(b), illustrates the process of tunneling from the left to the right lead, accompanied by two photon emissions. Note, that since the particle is being twice reflected by the EF in this process, the radiation, whatever strong, cannot suppress this channel of tunneling. The increase in the radiation power leads only to the enhancement of the transmission probability in the channel.

V. PHOTOCURRENT IN BALLISTIC SAMPLES

A. Photocurrent due to effectively two-dimensional modes

For the experimentally relevant parameters (see Sec. VII for more details), the electron Fermi momentum in the leads is much larger than the characteristic transverse momentum needed for a particle to be reflected at the p-n interface,

$$p_F \gg \sqrt{\frac{\hbar F_0}{\pi v}}. \quad (5.1)$$

Hence, the majority of the particles are in the “2D-modes”. In this subsection we calculate the photocurrent in a ballistic graphene p-n junction, neglecting the normal modes.

As we have just shown for such modes, the tunneling from left to right in a monotonically increasing potential is necessarily accompanied by the emission of one photon. Since the tunneling from left to right involves photon emission, tunneling from right to left, due to the time-reversal symmetry, involves photon absorption.

Then for some energies

$$P_{LR}(\varepsilon, \varepsilon - \hbar\Omega, \theta) \neq P_{LR}(\varepsilon - \hbar\Omega, \varepsilon, \theta) = 0, \quad (5.2)$$

and, according to the results of Section II, the photocurrent flows through the junction in absence of any voltage applied to it.

If the height of the potential obeys the inequality $U_0 > \hbar\Omega/2$, then at least one of the processes in the Fig. 5 or Fig. 6 or time-reversed processes is possible in the p-n junction, and some photocurrent flows through it. From now on we assume, however, that the barrier height and the Fermi energy are large enough,

$$\varepsilon_F > \hbar\Omega, \quad (5.3)$$

$$U_0 - \varepsilon_F > \hbar\Omega. \quad (5.4)$$

As it will be clear from the further consideration, under these conditions the photocurrent is maximal.

Since we are neglecting normal modes, and in the “2D-modes” the tunneling from left to right is possible only with a single-photon absorption, in Eq. (2.7) we have to discard all the terms except those with $n = -1$. Then,

according to Eq. (2.7), only the electrons with energies ε in the left lead, such that $\varepsilon - \hbar\Omega < \varepsilon_F < \varepsilon$, or, the same, $\varepsilon_F < \varepsilon < \varepsilon_F + \hbar\Omega$, contribute to the current.

This can be understood as follows. Each electron with energy $\varepsilon_F - \hbar\Omega < \varepsilon' < \varepsilon_F$ in the right lead penetrates into the left lead increasing its energy by $\hbar\Omega$ (Fig. 9). The current, carried by these electrons, is not compensated by the corresponding time-reversed processes, since the states of electrons, incoming from the left lead on the energies $\varepsilon_F < \varepsilon < \varepsilon_F + \hbar\Omega$ above the Fermi level, are unoccupied. So, the electrons coming from the leads on the correspondingly lower energies either compensate each others' contributions to the currents or return back to their initial leads.

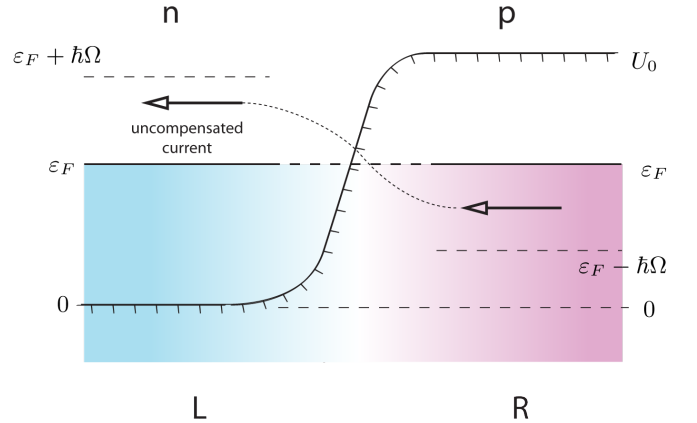


FIG. 9: (Color online) Contribution of electrons with different energies into the photocurrent through graphene p-n junction.

Thus, in order to find the photocurrent in the junction, one has to apply Eq. (2.7), performing integration over the states of the left lead with energies in the interval $(\varepsilon_F; \varepsilon_F + \hbar\Omega)$.

Let us assume that at some place around the resonant points the potential has a constant slope F . Then, according to the results of Section III, the probability for an electron at some energy ε and angle of incidence θ to go along the trajectory under consideration, is

$$P_{LR}(\varepsilon, \varepsilon - \hbar\Omega, \theta) = T(1 - T) = e^{-\mathcal{L} \cos \gamma} (1 - e^{-\mathcal{L} \cos \gamma}), \quad (5.5)$$

where γ is the angle between the electron momentum at the resonant point and the normal to the junction [cf. Figs. 5(b) and 6(b)], \mathcal{L} is the parameter introduced by Eq. (3.20).

According to Eq. (2.7) the photocurrent is

$$I_{2D} = 4W \int_{\varepsilon_F/v}^{(\varepsilon_F + \hbar\Omega)/v} dp \int_{-\arcsin \frac{\hbar\Omega}{2pv}}^{\arcsin \frac{\hbar\Omega}{2pv}} \frac{p d\theta}{(2\pi\hbar)^2} e v \cos \theta \times 2e^{-\mathcal{L} \cos \gamma(p, \theta)} (1 - e^{-\mathcal{L} \cos \gamma(p, \theta)}) \quad (5.6)$$

The angle γ can be determined from the transverse momentum conservation law

$$p \sin \theta = \frac{\hbar \Omega}{2v} \sin \gamma. \quad (5.7)$$

Then

$$I_{2D} = 4eW \int_{\varepsilon_F/v}^{(\varepsilon_F + \hbar \Omega)/v} dp \int_{-\pi/2}^{\pi/2} d\gamma \frac{\hbar \Omega}{(2\pi \hbar)^2} \cos \gamma \times e^{-\mathcal{L} \cos \gamma} (1 - e^{-\mathcal{L} \cos \gamma}) \quad (5.8)$$

$$= \frac{eW\Omega^2}{\pi v} (L_1(\mathcal{L}) - I_1(\mathcal{L}) - L_1(2\mathcal{L}) + I_1(2\mathcal{L})), \quad (5.9)$$

where $L_1(z)$ and $I_1(z)$ are correspondingly the modified Struve and the modified Bessel functions of the first order⁴⁵.

According to the Eqs. (3.20) and (3.5), the parameter \mathcal{L} is proportional to the intensity S of the EF:

$$\mathcal{L} = \frac{\pi^2 e^2 v S}{\hbar c F \Omega^2}. \quad (5.10)$$

Expression (5.9) is plotted in Fig. 10,

$$I_0 = \frac{eW\Omega^2}{v}. \quad (5.11)$$

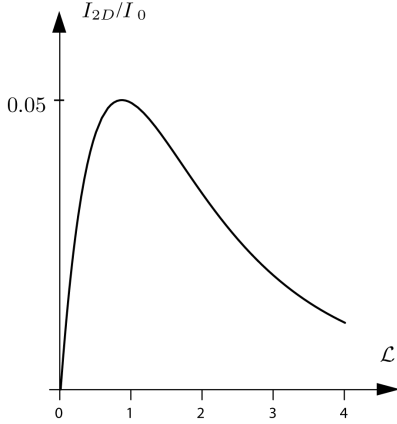


FIG. 10: Photocurrent in a graphene p-n junction as a function of the radiation intensity.

Small-intensity regime.

In the experimentally relevant regime of small radiation intensities ($\mathcal{L} \ll 1$) the photocurrent is

$$I_{2D}^{small} = \frac{eW\Omega^2}{2\pi v} \mathcal{L}. \quad (5.12)$$

The last formula can be understood as follows. The effective number of conducting “2D-modes”, i.e. of transverse channels in the energy interval $\sim \hbar \Omega$, is

$$N_{2D} = W \frac{\Omega}{v}. \quad (5.13)$$

The probability to tunnel in each channel, i.e., along each trajectory in the Figs. 5(b) and 6(b), is \mathcal{L} , in the limit of small \mathcal{L} . Then the Landauer-type conductance of each channel is $G = \frac{e^2}{h} \mathcal{L}$. Since each electron acquires the energy $\hbar \Omega$ tunneling from right to left, the effect of radiation on the conducting channels is equivalent to the effective voltage $V_{eff} = \hbar \Omega / e$ applied to the junction. Then Eq. (5.12) transforms into

$$I_{2D}^{small} = N_{2D} G V_{eff}. \quad (5.14)$$

Large-intensity regime.

In the limit of large radiation powers ($\mathcal{L} \gg 1$) Eq. (5.9) reduces to

$$I_{2D}^{large} = \frac{3eW\Omega^2}{4\pi^2 v} \frac{1}{\mathcal{L}^2}. \quad (5.15)$$

The photocurrent due to the modes under consideration is being suppressed by strong radiation, since the electrons tend to be reflected at each resonant point when \mathcal{L} is large and the tunneling along the paths in the Figs. 5(b) and 6(b) becomes unlikely.

Since the photocurrent carried by electrons with sufficiently large transverse momenta vanishes at $\mathcal{L} \rightarrow \infty$, one needs to consider the contribution of the other electrons incident almost normally at the p-n interface.

B. Photocurrent due to normal modes

In the normal modes electrons have very small transverse momenta p_{\perp} , so the problem can be viewed as one-dimensional. Introduce the effective number of normal modes, i.e. of the channels where electrons propagate without reflection at the p-n interface (taking into account spin and valley degeneracies):

$$N_{1D} = 4 \frac{W}{2\pi \hbar} \int_{-\infty}^{\infty} dp_{\perp} e^{-\frac{\pi p_{\perp}^2 v}{\hbar F_0}} = \frac{2W}{\pi \hbar} \sqrt{\frac{\hbar F_0}{v}}. \quad (5.16)$$

As discussed before, when the condition (5.1) is satisfied, one has the inequality $N_{2D} \gg N_{1D}$.

The corresponding effective one-dimensional density of states (per a unit of longitudinal length) is

$$\nu_{1D} = \frac{N_{1D}}{2\pi \hbar v}. \quad (5.17)$$

The current, flowing through the junction within the one-dimensional picture, is³⁷ [cf. also Eq. (2.7)]

$$I = \int d\varepsilon \nu_{1D} \sum_n P_{LR}(\varepsilon, \varepsilon + n\hbar \Omega) \times (f_L^{in}(\varepsilon) - f_R^{in}(\varepsilon + n\hbar \Omega)), \quad (5.18)$$

where $P_{LR}(\varepsilon, \varepsilon + n\hbar \Omega)$ is the probability to tunnel from left to right from the state with energy ε to the one with $\varepsilon + n\hbar \Omega$.

The only tunneling process contributing to the photocurrent [Fig. 8(b)] is the one when the particle is being reflected at both resonant points, emitting two photons. The probability of this double reflection is $(1 - e^{-\mathcal{L}})^2$.

The photocurrent due to the normal modes is possible provided $U_0 > \hbar\Omega$. Again, we assume that the height of the potential barrier and the Fermi level are large enough, so that the photocurrent due to the processes under consideration not simply exists, but also reaches maximum as a function of these parameters,

$$\varepsilon_F > \frac{3\hbar\Omega}{2}, \quad (5.19)$$

$$U_0 - \varepsilon_F > \frac{3\hbar\Omega}{2}, \quad (5.20)$$

so that both resonant points are present on the potential for each electron in the energy interval of the width $2\hbar\Omega$.

Then the photocurrent due to the normal modes is

$$I_{1D} = \frac{e^2}{h} (1 - e^{-\mathcal{L}})^2 \left(\frac{2\hbar\Omega}{e} \right) N_{1D}. \quad (5.21)$$

We see thus, that at very large intensities ($\mathcal{L} \gg 1$) the photocurrent is saturated. This happens because in this limit any electron, reflected twice by the radiation with the probability close to 1, recovers its initial direction of velocity and penetrates into the opposite lead.

C. Full current vs. radiation intensity

To sum up, the full photocurrent I flowing through the irradiated p-n junction is given by the sum

$$I = I_{2D} + I_{1D} \quad (5.22)$$

with I_{2D} and I_{1D} given by Eqs. (5.9) and (5.21) respectively.

If the radiation power is not too large,

$$\mathcal{L}^2 \lesssim \frac{3}{4\pi} \frac{N_{2D}}{N_{1D}}, \quad (5.23)$$

the p-n junction is effectively two-dimensional, and the photocurrent in it is described by Eq. (5.9). For larger intensities, when the last inequality reverts, the photocurrent strongly decreases (by the factor of $\sim N_{2D}/N_{1D}$) and saturates at the value $I_{1D}(\mathcal{L} \rightarrow \infty) = e\hbar\Omega N_{1D}/\pi$.

D. Suppression of the tunneling

Current-voltage characteristic of a strongly irradiated junction. Assume now that the voltage V is applied to the junction. Here we make the convention that the voltage is positive in the case of the forward bias, when the electric potential of the p-type graphene is larger than that of the n-type. The corresponding direction of the current in the absence of radiation is considered positive.

Introducing the conductance G_{ball} of the ballistic graphene p-n junction

$$G_{ball} = \frac{e^2}{h} N_{1D}, \quad (5.24)$$

and taking into account Eq. (5.21), the current-voltage characteristic of the junction under a very strong irradiation ($\mathcal{L}^2 \gg N_{2D}/N_{1D}$) can be written as

$$I(V) = G_{ball} \left(V - \frac{2\hbar\Omega}{|e|} \right). \quad (5.25)$$

The second term in the parenthesis of the last equation is the photocurrent, Eq. (5.21) written in the limit $\mathcal{L} \rightarrow \infty$. The equation holds until $V < U_0 - \varepsilon_F + \hbar\Omega/2$. For larger voltages the current grows even more rapidly due to the appearance of normal modes without resonant points.

Thus, the current through the p-n junction with high enough potential barrier cannot be suppressed by the radiation, due to the existence of the channels where electrons can tunnel with probability 1, gaining or losing two quanta $\hbar\Omega$. As a result, the differential conductance of the junction is the same as in the absence of radiation.

Conditions for tunneling suppression.

In order to suppress the tunneling in the junction one has to cancel the photocurrent due to the ‘‘1D modes’’, i.e. to make a sufficiently low potential barrier $U_0 < \hbar\Omega$ (or increase the frequency), such that the normal trajectories with two resonant points no longer exist.

Making a p-n junction with $U_0 > \hbar\Omega/2$ and with one resonant point for electrons coming with the Fermi energy, and then applying strong radiation one can exponentially suppress the conductance due to the normal modes and suppress the photocurrent carried by the ‘‘2D modes’’, because it becomes proportional to $\propto \mathcal{L}^{-2}$, Eq. (5.15). One may also think of the situation for $U_0 < \hbar\Omega/2$ when one resonant point still exists for electrons coming at the Fermi energy. In that case, applying a small voltage V to the junction, one obtains the normal current $I \sim I_{2D}^{large}(eV/\hbar\Omega) \sim (e^2 W \Omega V / v \hbar) \mathcal{L}^{-2}$, which is also suppressed at large intensities as $\propto \mathcal{L}^{-2}$.

VI. PHOTOCURRENT IN DISORDERED SAMPLES

In the previous sections we considered purely ballistic quasiparticle transport in irradiated graphene samples. In principle, the transport can be strongly affected by disorder, electron-phonon and electron-electron interactions. According to the Ref. 46, as concerns their conductance, junctions fabricated in recent experiments are at the best in the crossover between the ballistic and diffusive regimes.

In this section we calculate the photocurrent in a p-n junction under a weak irradiation, $\mathcal{L} \ll 1$, in a disordered sample in presence of electron-electron interaction. We show that the photocurrent is the same as previously

calculated in a ballistic sample, Eq. (5.12), provided that the impurities-induced resistance of some resonant region in the junction, where the carriers are effectively excited by the radiation, is not large compared to the ballistic resistance of the junction.

In this section we use the following assumptions. We neglect the relaxation due to electron-phonon interaction on the length of the junction and assume that the condition (3.23) is fulfilled. The validity of such approximations will be confirmed in Sec. VII by explicit estimates. For simplicity, we suppose that the intervalley scattering is weak and neglect it. Taking this scattering into account is possible in a similar way, which leads to the similar formulas. When writing the kinetic equations we also neglect the possibility of disorder-assisted photon emission or absorption. In fact, electrons can rebound from the impurities, gaining or losing energy quanta $\hbar\Omega$ in the same way as from the smooth potential $U(\mathbf{r})$, considered in Sec. III. Such a process would open additional channels for the tunneling of electrons from one lead into the another and thus would increase the photocurrent.

Introduce the distribution function of electrons in the conduction band, $f_{\uparrow}(\mathbf{p}, \mathbf{r}, t)$, and in the valence band, $f_{\downarrow}(\mathbf{p}, \mathbf{r}, t)$. The first ones have their momenta parallel to their pseudospins, while the second- antiparallel. The stationary distributions are described by the kinetic equations (for the derivation see the Appendix)

$$\left(-\partial_{\mathbf{r}}U\partial_{\mathbf{p}} + v\frac{\mathbf{p}}{p}\partial_{\mathbf{r}}\right) f_{\uparrow} = \Gamma(\mathbf{p})(f_{\downarrow} - f_{\uparrow}) + (\text{St}f)_{\uparrow}, \quad (6.1)$$

$$\left(-\partial_{\mathbf{r}}U\partial_{\mathbf{p}} - v\frac{\mathbf{p}}{p}\partial_{\mathbf{r}}\right) f_{\downarrow} = \Gamma(\mathbf{p})(f_{\uparrow} - f_{\downarrow}) + (\text{St}f)_{\downarrow}, \quad (6.2)$$

where $\Gamma(\mathbf{p})$ is the rate of the radiation-induced pseudospin-flips, and

$$\text{St}f = (\text{St}f)^{imp} + (\text{St}f)^{ee} \quad (6.3)$$

is the collision integral for impurity scattering and electron-electron interaction.

Kinetic equations (6.1), (6.2) are valid in the case of weak enough radiation, $\mathcal{L} \ll 1$. The effect of the radiation and the effect of other processes on the electron dynamics are described by two independent terms in the right-hand sides (rhhs) of the equations. The mutual influence of the two corresponding transition rates on each other can be neglected due to the fulfillment of the condition (3.23), derived in Sec. III from the considerations of Landau-Zener tunneling in the momentum space. The same condition, [A24], follows from the explicit derivation of the kinetic equations (cf. Appendix). Let us emphasize, that treating perturbatively the effect of disorder and radiation-induced transitions in Eqs. (6.1) and (6.2) one should use the values of velocity v and collisional terms, renormalized by disorder⁴⁷ and electron-electron interactions⁴⁸.

The contribution of elastic impurities into the collision integral has the form

$$(\text{St}f_{\uparrow,\downarrow}(\mathbf{p}, \mathbf{r}))^{imp}$$

$$= \int d\mathbf{p}' w_{\mathbf{p}\mathbf{p}'} (f_{\uparrow,\downarrow}(\mathbf{p}', \mathbf{r}) - f_{\uparrow,\downarrow}(\mathbf{p}, \mathbf{r})) \delta(p - p'), \quad (6.4)$$

where the quantity $w_{\mathbf{p}\mathbf{p}'}$ satisfies the condition following from the time-reversal symmetry

$$w_{\mathbf{p}\mathbf{p}'} = w_{\mathbf{p}'\mathbf{p}}, \quad (6.5)$$

similarly to the analogous Eq. (2.6) in Sec. II.

Analogously one can write the collision integral $(\text{St}f)^{ee}$ for the electron-electron interaction (see, for instance, Ref. 48). However, further we will not need an explicit form of this integral using instead only the fact that the electron-electron interaction does not considerably modify the resistance of the junction, i.e. that such a modification is much smaller than the ballistic resistance of the junction.

We derive the photocurrent from the kinetic equations (6.1), (6.2), making perturbation theory in $\Gamma(\mathbf{p})$. In the zeroth order, when $\Gamma(\mathbf{p}) = 0$, neglecting the change of the distribution functions due to the collision integral on the energy scales of order of ε_F and $\hbar\Omega$, we can write the solution of Eq. (6.1) as an equilibrium Fermi distribution $f_{\uparrow}^0(\mathbf{p}, \mathbf{r}, t) = \theta(\varepsilon_F - vp - U(\mathbf{r}))$, where θ is the theta-function. Similarly, the solution of Eq. (6.2) in absence of radiation is $f_{\downarrow}^0(\mathbf{p}, \mathbf{r}, t) = \theta(\varepsilon_F + vp - U(\mathbf{r}))$.

Taking into account the processes of the first order in $\Gamma(\mathbf{p})$, one arrives at a slightly modified version of these distributions; the radiation excites some small number of electrons with energies $\varepsilon_F - \hbar\Omega < \varepsilon' < \varepsilon_F$ into the energy interval $\varepsilon_F < \varepsilon < \varepsilon_F + \hbar\Omega$. This happens sufficiently close to the p-n interface, at $|U(z) - \varepsilon_F| < \hbar\Omega/2$ (see Fig. 11).

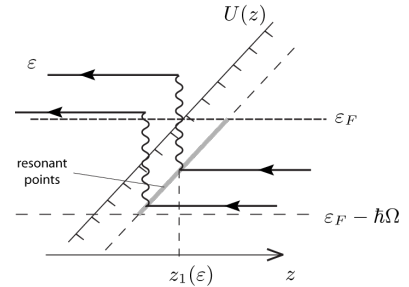


FIG. 11: Radiation-induced excitation processes, which contribute to the photocurrent in the graphene p-n junction.

Since above the Fermi energy the distribution function f is small, $f \ll 1$, and below- $f \approx 1$, we can rewrite Eq. (6.1) for the electrons in the valence band in the aforementioned region as

$$\left(-\partial_{\mathbf{r}}U\partial_{\mathbf{p}} + v\frac{\mathbf{p}}{p}\partial_{\mathbf{r}}\right) f_{\uparrow} = \Gamma(\mathbf{p}) + (\text{St}f)_{\uparrow}. \quad (6.6)$$

Let us multiply this equation by the factor $4pe d\varepsilon d\theta/(h^2v)$ and integrate over the angle θ or, in other words, over the direction of momentum \mathbf{p} . Introduce

$$\bar{\Gamma} = \frac{\pi\Delta^2}{\hbar} \delta(\hbar\Omega - 2pv), \quad (6.7)$$

which is the rate $\Gamma(\mathbf{p})$, averaged over the direction of \mathbf{p} , and $\nu_0 = \Omega/(\pi\hbar v^2)$, the density of states per unit square at the resonant point (the latter takes into account spin and valley degeneracies). From Eq. (6.6) we get after the integration

$$\text{div} \left(\frac{\partial \mathbf{j}_\uparrow(\varepsilon, z)}{\partial \varepsilon} d\varepsilon \right) = e\bar{\Gamma}\nu_0 d\varepsilon + e \left(\frac{\partial}{\partial t} \frac{\partial n_\uparrow}{\partial \varepsilon} \right)^{ee} d\varepsilon, \quad (6.8)$$

where

$$\frac{\partial n_\uparrow(\varepsilon, z)}{\partial \varepsilon} d\varepsilon = d\varepsilon \cdot 4 \int \frac{p d\theta}{(2\pi\hbar)^2 v} f_\uparrow(t, \mathbf{p}, z) \quad (6.9)$$

and

$$\frac{\partial j_\uparrow(\varepsilon, z)}{\partial \varepsilon} d\varepsilon = d\varepsilon \cdot 4e \int \frac{\mathbf{p} d\theta}{(2\pi\hbar)^2} f_\uparrow(t, \mathbf{p}, z) \quad (6.10)$$

are correspondingly the density of electrons and the density of the current, carried by electrons with energies in the interval $(\varepsilon, \varepsilon + d\varepsilon)$ in the conduction band at the coordinate point z . The last term in Eq. (6.8) describes the change of the density of electrons due to electron-electron interactions.

Note, that due to the condition (6.5), the contribution (6.4) of elastic impurities into the collision integral disappears in Eq. (6.8) after the integration over the direction of \mathbf{p} . Indeed, Eq. (6.8) is the charge continuity equation for the carriers with energy in the interval $d\varepsilon$, and the elastic scatterers cannot affect the corresponding charge density. The two terms in the right-hand side of Eq. (6.8) represent the two inelastic processes changing the density $(\partial n_\uparrow/\partial \varepsilon)d\varepsilon$: external radiation and electron-electron interaction.

The total current through the junction is given by the integral of the current density over the energy:

$$I_{ph} = W \int_{\varepsilon_F - \hbar\Omega}^{\varepsilon_F + \hbar\Omega} \left(\frac{\partial j_\uparrow(\varepsilon, z)}{\partial \varepsilon} + \frac{\partial j_\downarrow(\varepsilon, z)}{\partial \varepsilon} \right) d\varepsilon. \quad (6.11)$$

Depending on the coordinate point z , it can be carried either by the particles in the conduction band or in the valence band or both.

When the junction is non-ballistic, the photocurrent depends on the resistances of different parts of the junction and of the leads. Let us calculate the photocurrent, assuming that the impurities are present only in the ‘‘resonant region’’, $|U(z) - \varepsilon_F| < \hbar\Omega/2$, while outside this region they are absent, and the transport is purely ballistic. The parts of the junction outside this region in the leads can be considered as some external circuit, the resistance of which can be easily taken into account after we obtain the final result for the photocurrent.

Integrating Eq. (6.8) over the longitudinal coordinate z , we obtain

$$\frac{\partial j_\uparrow(\varepsilon, z_1 + 0)}{\partial \varepsilon} - \frac{\partial j_\uparrow(\varepsilon, z_1 - 0)}{\partial \varepsilon} = \frac{1}{2} \mathcal{L} e \nu \nu_0, \quad (6.12)$$

$$\frac{\partial j_\uparrow(\varepsilon, z)}{\partial \varepsilon} = e \int_{z_1(\varepsilon)}^z \left(\frac{\partial}{\partial t} \frac{\partial n_\uparrow}{\partial \varepsilon} \right)^{ee} dz + \text{const}_1,$$

$$z > z_1, \quad (6.13)$$

$$\frac{\partial j_\uparrow(\varepsilon, z)}{\partial \varepsilon} = e \int_{z_1(\varepsilon)}^z \left(\frac{\partial}{\partial t} \frac{\partial n_\uparrow}{\partial \varepsilon} \right)^{ee} dz + \text{const}_2, \quad (6.14)$$

$$z < z_1,$$

where $z_1(\varepsilon)$ is the resonant point, corresponding to the energy ε .

Electron-electron collisions conserve the total density of particles $n(z) = \int (\partial n_\uparrow/\partial \varepsilon + \partial n_\downarrow/\partial \varepsilon) d\varepsilon$ at a given point z , which leads to the relation

$$\int d\varepsilon \left[\left(\frac{\partial}{\partial t} \frac{\partial n_\uparrow}{\partial \varepsilon} \right)^{ee} + \left(\frac{\partial}{\partial t} \frac{\partial n_\downarrow}{\partial \varepsilon} \right)^{ee} \right] = 0. \quad (6.15)$$

If the ballistic resistance of the junction is much larger than the characteristic diffusive resistance induced by impurities and electron-electron interaction in the resonant region,

$$R_{ball} \gg R_{diff}, \quad (6.16)$$

one can show, that the transmission of particles with energy ε through the point $z_0(\varepsilon)$, such that $U(z_0) = \varepsilon$, is still strongly impeded, and the photocurrent (6.11) in the conduction and the valence band is given mainly by the currents $\frac{j_\uparrow(\varepsilon, z_1 - 0)}{\partial \varepsilon} d\varepsilon$ and $\frac{\partial j_\downarrow(z_1 + 0)}{\partial \varepsilon} d\varepsilon$, as shown in Fig. 11.

Indeed, if dn_\uparrow is the density of excited electrons in the energy interval $d\varepsilon$ in the resonant region, then, for instance, the current density

$$\frac{\partial j_\uparrow(\varepsilon, z_1 - 0)}{\partial \varepsilon} \sim \frac{\partial n_\uparrow/\partial \varepsilon}{eW R_{diff} \nu_0} \quad (6.17)$$

is much larger than

$$\frac{\partial j_\uparrow(\varepsilon, z_1 + 0)}{\partial \varepsilon} \sim \frac{\partial n_\uparrow/\partial \varepsilon}{eW(R_{diff} + R_{ball})\nu_0}, \quad (6.18)$$

since the condition (6.16) is fulfilled.

Taking into account the condition

$$\frac{\partial j_\uparrow(\varepsilon, z_1 - 0)}{\partial \varepsilon} \gg \frac{\partial j_\uparrow(\varepsilon, z_1 + 0)}{\partial \varepsilon} \quad (6.19)$$

and Eq. (6.15), one can find the photocurrent by integrating the current density at some point z on the left from the resonant point:

$$I_{ph} \approx W \int_{\varepsilon_F}^{\varepsilon_F + \hbar\Omega} \frac{\partial j_\uparrow(\varepsilon, z)}{\partial \varepsilon} d\varepsilon \quad (6.20)$$

$$= \frac{1}{2} \mathcal{L} e \nu \nu_0 \hbar\Omega = \frac{eW\Omega^2}{2\pi v} \mathcal{L}, \quad (6.21)$$

the same result as given by the Eq. (5.12).

Thus, we have shown that in a disordered sample, where the ballistic considerations of the previous sections cannot be immediately applied due to the presence of elastic impurities and electron-electron interaction in the resonant region, the photocurrent does not change until

the disorder or the interactions become too strong, so that the impurities-induced or the interactions-induced resistance becomes larger than the ballistic one.

In the opposite limit, $R_{diff} \gg R_{ball}$, the excited electrons and holes, created in the resonant region by the radiation, diffuse almost independently of the external potential at the p-n interface. The effect of large diffusive resistance of the resonant region on the photocurrent is analogous to the effect of a large resistance of the external circuit. The photocurrent in this regime is reduced as

$$I_{ph}^{diff} \sim \frac{R_{ball}}{R_{diff}} I_{ph}, \quad (6.22)$$

with I_{ph} given by Eq. (6.21).

According to the Ref. 46, in the recent experiments^{12,13} the ballistic resistance is of the same order of magnitude as the diffusive one, defined as a difference between the resistances of n-n and p-n junctions. If $R_{ball} \sim R_{diff}$, Eq. (6.21) is only an order-of-magnitude estimate of the photocurrent. As follows from the derivation of the photocurrent, the increase of the resistance R_{diff} leads to the decrease of the photocurrent. One can make the resistance R_{diff} smaller than the ballistic resistance, decreasing the frequency of the EF and thus reducing the size of the resonant region and R_{diff} .

VII. POSSIBILITY OF EXPERIMENTAL OBSERVATION OF PHOTOCURRENT

In this section we address the question of experimental observability of the photocurrent in a graphene p-n junction. We analyze the necessary conditions and estimate the value of the photocurrent for achievable radiation intensities and the junction parameters.

Geometrical parameters and gate voltages. As discussed in the previous section, for the largest photocurrent one needs the diffusive resistance of the junction to be smaller than the ballistic one. This can be achieved by using sufficiently short junctions⁴⁶. Let us take the length of the junction $L = 100nm$, close to that in the experiment in Ref. 12, where the resistance of the junction is described by the ballistic model rather than by the diffusive one. The typical width W of a p-n junction^{11,12,13,14} is a few micrometers; for our estimates we take $W = 1\mu m$.

Let $U_0 = 0.4eV$ and $\varepsilon_F = U_0/2$ be, respectively, the height of the potential barrier and the Fermi energy, close to the typical experimental parameters. For the slope of the potential we use the naive estimate $F = U_0/L$, regarding it as constant along the junction. To be more precise, considering the effective potential, one should take into account the non-uniform charge density distribution in the junction⁴⁴. However, the corrected in such a way potential profile would have the slope of the same order of magnitude as the naive estimate.

Characteristic relaxation lengths.

For the chosen parameters of a junction the characteristic length of Landau-Zener tunneling, given by Eq. (3.22), is

$$\Delta r_{LZ} \sim \sqrt{\frac{\hbar v}{F}} \approx 13nm. \quad (7.1)$$

According to the experiment in Ref. 49, where the relaxation time of carriers excited by the near-infrared light has been measured, electron-electron interaction is responsible for the fastest stage of relaxation, occurring on the typical time $\sim 0.1ps$, corresponding to the electron path $l_{ee} \sim 0.1\mu m$. Since $l_{ee} \gg \Delta r_{LZ}$, the condition (3.23) is fulfilled, as we assumed in the previous section. Another slower stage of relaxation due to the electron-phonon interaction has a characteristic length $\sim 1\mu m$.

The mean free path of carriers in graphene is of order of $1\mu m$ at room temperature^{1,4}. The characteristic length of relaxation due to electron-phonon interaction should be of the same order or larger. Then the neglect of such a relaxation in the previous section is quite a reasonable approximation.

Desirable radiation frequency. Calculating the current due to “2D-modes” in the Sec. V, we dealt with momentum scales much larger than $p_{\perp}^0 = (\hbar F/\pi v)^{\frac{1}{2}}$. Accordingly, to have resonant points on the electron trajectories in the “2D-modes”, one should apply the radiation with angular frequency Ω much larger than

$$\Omega_{ir} = \frac{p_{\perp}^0 v}{\hbar} = \left(\frac{vF}{\pi\hbar}\right)^{\frac{1}{2}}. \quad (7.2)$$

If $\Omega \lesssim \Omega_{ir}$, then the “2D-modes” and some “1D-modes” do not have resonant points, that is, there exist electrons only weakly affected by the EF and freely penetrating through the p-n interface without reflection. As a result, if the frequency Ω is too low, the photocurrent is strongly reduced, and the suppression of tunneling is impossible.

Note, that according to the Eqs. (5.16) and (5.13) the condition $\Omega \gg \Omega_{ir}$ is equivalent to $N_{2D} \gg N_{1D}$, ensuring that the junction is effectively two-dimensional. Provided this condition is fulfilled, the current is carried mainly by the “2D-modes”. For our choice of junction parameters $\hbar\Omega_{ir} \approx 29meV$, which corresponds to the frequency $f_{ir} = \Omega_{ir}/(2\pi) \approx 7THz$.

As we noted in the Sec. V, the photocurrent is possible if $U_0 > \hbar\Omega/2$, i.e. $\hbar\Omega < 800meV$ (or $\Omega < 200THz$). However, to maximize the photocurrent one should satisfy conditions (5.3) and (5.4), for the case under consideration equivalent to $\hbar\Omega < U_0/2 = 200meV$.

Magnitude of the photocurrent. The characteristic radiation intensity used in the experiments with nanotube junctions^{23,25} is about a few kW/cm^2 . Assume, the same intensities can be applied to graphene junction, and set $S = 10kW/cm^2$, close to the maximal value reached in Ref. 23.

Then the photocurrent is

$$I = \frac{\pi e^3 W}{2\hbar c F} S \approx 0.3\mu A, \quad (7.3)$$

independently of the frequency in the desirable range $\hbar\Omega_{ir} < \hbar\Omega < U_0/2$. Note, that the photocurrent is a few orders of magnitude larger than those obtained in the experiments with carbon nanotubes^{22,23,24}.

Possibility of tunneling suppression. To maximize the dynamical gap, Eq. (3.5), one should lower the frequency. For $\hbar\Omega = \hbar\Omega_{ir} = 29meV$ we obtain the dynamical gap $\Delta \approx 6meV$ and the exponent of tunneling through it— $\mathcal{L} \approx 10^{-3}$, which is insufficient to suppress the tunneling. To confine electrons, i.e. to achieve $\mathcal{L} \gg 1$, one should use proportionally larger radiation powers or longer junctions.

VIII. CONCLUSION

To sum up, we studied electron transport in graphene junctions irradiated by monochromatic electromagnetic field (EF).

The radiation opens dynamical gaps in the quasiparticle spectra, proportional to the amplitude of the EF and inversely proportional to its frequency, Eq. (3.5). The appearance of the gaps results in a strong modification of current-voltage characteristics of a junction.

If the height of the potential barrier is large enough, the directed current (*photocurrent*), Eq. (5.9), flows through the junction without any dc bias voltage applied. At small radiation intensities, the photocurrent, proportional to the radiation power, Eq. (5.12), is a result of inelastic quasiparticle tunneling assisted by one-photon absorption. At large intensities, the photocurrent, Eq. (5.15), decreases with radiation power and finally saturates at some constant value, Eq. (5.21).

When the potential barrier is smaller than the photon energy $\hbar\Omega$ but larger than $\hbar\Omega/2$, the saturation does not happen and the photocurrent decreases to zero at large radiation intensities. When the potential barrier is smaller than $\hbar\Omega/2$, any photocurrent is absent. In these regimes, one can adjust the Fermi level in such a way, that the quasiparticle transmission in the junction is determined by the tunneling through the gap and can be fully suppressed, provided that the radiation power is large enough.

In the present paper we also analyze the influence of elastic impurities and electron-electron interaction on the magnitude of the photocurrent, and show that they weakly affect the photocurrent, if the diffusive resistance of the junction is not too large compared to the ballistic one.

Acknowledgements. We thank L.I. Glazman, M.Yu. Kharitonov, and A.F. Volkov for useful discussions. This work has been financially supported by SFB Transregio 12 and SFB 491.

APPENDIX A: KINETIC EQUATION IN IRRADIATED GRAPHENE

Now we derive explicitly the kinetic equation, governing the dynamics of the electron distribution functions in graphene exposed to monochromatic electromagnetic wave, taking into account the effect of disorder, electron-electron and electron-phonon interactions on the transport. Since graphene in the vicinity of some resonant point can be considered as a semiconductor with the spectrum, linearized close to the resonant momentum, the dynamics of carriers, for which the radiation matters, should be the same as for conventional semiconductors^{50,51,52}.

As the radiation can only flip the pseudospin and does not induce intervalley scattering, deriving the kinetic equation in the lowest non-vanishing order in the radiation power, we can limit ourselves to the consideration of dynamics in a single valley and a single spin direction, because the intervalley- and spin- scattering would enter only the part of the collision integral, which is independent of the radiation.

It is convenient to perform calculations in the basis of electron states $|\uparrow_{\mathbf{p}}\rangle$, pseudospin is directed along the momentum \mathbf{p} , and $|\downarrow_{\mathbf{p}}\rangle$, pseudospin is antiparallel to \mathbf{p} . We choose correspondingly the coordinate system in the momentum space such that z axis is directed along \mathbf{p} and the x axis is perpendicular to \mathbf{p} and parallel to the graphene plane (the plane, in which \mathbf{p} can vary), and the y axis—normally to the plane. This frame fixes the pseudospin basis.

Since the basis depends explicitly on \mathbf{p} , in the momentum representation one should substitute in the Hamiltonian (3.2) the operator of spatial coordinate $\hat{\mathbf{r}}$ by the covariant momentum derivative:

$$\hat{\mathbf{r}} \rightarrow \tilde{\mathbf{r}} = i \frac{\partial}{\partial \mathbf{p}} + \frac{1}{2} \frac{\partial \alpha}{\partial \mathbf{p}} \hat{\sigma}_y, \quad (\text{A1})$$

where $\alpha(\mathbf{p})$ is the angle of rotation of the frame about the y axis, normal to the graphene plane. In this section $\hbar = 1$. The second term in the last expression is the gauge potential due to the local frame rotations in the momentum space.

The modulus of this term for a given momentum \mathbf{p} is of order of the corresponding Fermi wavelength $\lambda_F \sim (\partial\alpha/\partial p)$. Far from the Dirac point it is much smaller than the characteristic scale on which the potential $U(\mathbf{r})$ changes. This allows us to expand the potential up to the first order in the gauge field, and write the Hamiltonian as

$$\hat{\mathcal{H}} \approx vp\hat{\sigma}_z + U(\mathbf{r}) + (2p)^{-1}\partial_x U(\mathbf{r})\hat{\sigma}_y \quad (\text{A2})$$

in the basis chosen. Here $\partial_x U(\mathbf{r}, \mathbf{p}) = (dU(\mathbf{r})/d\mathbf{r})\mathbf{e}_x(\mathbf{p})$, \mathbf{e}_x is the unit vector directed along the perpendicular to momentum \mathbf{p} the x axis in the graphene plane.

Now let us proceed to the derivation of the kinetic equation for the distribution functions in the basis of

states $|\uparrow_{\mathbf{p}}\rangle, |\downarrow_{\mathbf{p}}\rangle$. Analogously to the field operator $\hat{\Psi} = (\hat{\Psi}_e, \hat{\Psi}_h^\dagger)^T$ in a conventional semiconductor⁵⁰, we introduce the operator $\hat{\Psi} = (\hat{\Psi}_\uparrow, \hat{\Psi}_\downarrow)^T$ with two components acting correspondingly in the conduction and the valence bands of graphene. In the momentum representation the indices \uparrow and \downarrow of the operator $\hat{\Psi}(\mathbf{p})$ refer to the particles with pseudospins aligned along or opposite to the momentum \mathbf{p} , respectively. Then we introduce the non-equilibrium Green's functions

$$G_{ab}^<(1, 2) = i\langle \hat{\Psi}_b^\dagger(2), \hat{\Psi}_a(1) \rangle, \quad (\text{A3})$$

$$G_{ab}^>(1, 2) = -i\langle \hat{\Psi}_a(1), \hat{\Psi}_b^\dagger(2) \rangle, \quad (\text{A4})$$

where $a, b = \uparrow, \downarrow$; $1 = \{t_1, \mathbf{r}_1\}$; $2 = \{t_2, \mathbf{r}_2\}$. Accordingly, we define⁵³ the 2×2 matrix Green's functions G^A , G^R , and G^K , and the matrix function

$$\underline{G} = \begin{pmatrix} G^R & G^K \\ 0 & G^A \end{pmatrix}, \quad (\text{A5})$$

which satisfies the equation⁵³

$$[(G_0^{-1} - \underline{\Sigma}) \otimes \underline{G}] = 0 \quad (\text{A6})$$

(Dyson equation minus its conjugate), where $G_0^{-1}(1, 1') = (i\partial_{t_1} - \varepsilon(1))\delta(1 - 1')$, ε is the Hamiltonian of the particles unperturbed by the radiation and impurities, and $\underline{\Sigma}$ is the self-energy. The square brackets here stand for the commutator $[A \otimes B] = A \otimes B - B \otimes A$.

Let us decompose $\underline{\Sigma}$ into two parts,

$$\underline{\Sigma}(1, 1') = \hat{V}(t_1)\delta(1 - 1') + \underline{\Sigma}_i(1, 1'), \quad (\text{A7})$$

where $\hat{V}(t)$ is the EF-induced perturbation of the single-particle Hamiltonian, $\underline{\Sigma}_i(1, 1')$ - the rest of the self-energy part. Assuming that the EF is weak and purposing to find the dynamics of the carries in the lowest order in the radiation power, we will neglect the effect of external radiation on $\underline{\Sigma}_i$.

It is convenient to solve the problem in the Wigner representation, introducing the ‘‘center of mass’’ coordinates $T = (t_1 + t_2)/2$, $\mathbf{R} = (\mathbf{r}_1 + \mathbf{r}_2)/2$ and the relative ones, $\tau = t_1 - t_2$, $\mathbf{r} = \mathbf{r}_1 - \mathbf{r}_2$, and making Fourier transform of all the Green's functions with respect to τ and \mathbf{r} .

However, unlike the usual situation⁵³, we expect that in the Wigner representation only the quantities

$$\begin{aligned} & \underline{G}_0^{-1}(T, \mathbf{R}, \mathbf{p}, \varepsilon) = \\ & = \varepsilon - vp\hat{\sigma}_z - U(\mathbf{R}) - (2p)^{-1}\partial_x U(\mathbf{R}, \mathbf{p})\hat{\sigma}_y, \end{aligned} \quad (\text{A8})$$

G_{aa}^K , and $\underline{\Sigma}_i$ are the slow functions of time T , i.e. vary on the time scales much larger than the inversed relevant kinetic energies of electrons, while the other functions, $G^{A/R}$ and G_{ab}^K , contain contributions proportional to the fast in T perturbation $\hat{V}(T) = -(ev/c)\mathbf{A}(T)\hat{\sigma}$. The diagonal elements G_{aa}^K of the Keldysh Green's function should be slow since they depend only on the electron distribution function, which should vary slowly due

to the weakness of perturbation. Below we confirm this by the direct calculation.

In order to derive the kinetic equation, we consider the Keldysh component of Eq. (A6):

$$\begin{aligned} & [G_0^{-1} \otimes G^K] = [\hat{V} \otimes G^K] \\ & + \Sigma_i^R \otimes G^K - G^K \otimes \Sigma_i^A + \Sigma_i^K \otimes G^A - G^R \otimes \Sigma_i^K. \end{aligned} \quad (\text{A9})$$

Taking into account the slowness of G^K , one can rewrite the left part of the last equation using the gradient approximation⁵³:

$$\begin{aligned} & i \left(\partial_T G^K - \partial_{\mathbf{R}} U \partial_{\mathbf{p}} G^K \frac{1}{2} \left\{ \frac{\mathbf{p}}{p} v \hat{\sigma}_z, \partial_{\mathbf{R}} G^K \right\} \right. \\ & \left. + i[vp\hat{\sigma}_z, G^K] + (2p^{-1})\partial_x U [\hat{\sigma}_y, G^K] \right) \\ & = [\hat{V} \otimes G^K] + \Sigma_i^R \otimes G^K - G^K \otimes \Sigma_i^A \\ & \quad + \Sigma_i^K \otimes G^A - G^R \otimes \Sigma_i^K. \end{aligned} \quad (\text{A10})$$

The brackets $[\cdot, \cdot]$ stand here for the commutators of matrices, $\{\cdot, \cdot\}$ - for the anticommutators. The left part of the last equation describes the ballistic properties of electrons in graphene. The last four terms describe the change of distribution functions due to the electron scattering, independent of the radiation. Further we do not consider these terms in detail and focus on the radiation-induced transitions, i.e. on the first term in the right-hand side of Eq. (A10). We will only assume, that the rate of the radiation-independent scattering between the states $|\uparrow_{\mathbf{p}}\rangle$ and $|\downarrow_{\mathbf{p}}\rangle$ is not too strong compared to the rate of the radiation-induced transitions, so that the latter can be calculated independently. The applicability of this assumption will be discussed below.

The term $[(\partial_x U/2p)\hat{\sigma}_y, G^K]$ in the left-hand side of Eq. (A10) can be rewritten into the right-hand side (rhs) as $-(\partial_x U/2p)[\hat{\sigma}_y \otimes G^K]$ in the leading order in the gradient approximation. Then the term $-(\partial_x U/2p)\hat{\sigma}_y$ can be considered in the further calculations as an additional small perturbation, induced by the electromagnetic field with frequency and amplitude going to zero [cf. Eq. (3.3)]. Such a perturbation could induce transitions between electron states close to the Dirac point. However, here we are interested in the radiation-induced transitions between the states with large momenta close to the resonant ones. Then we will disregard the last term in the left-hand side of Eq. (A10). Within such an approximation the kinetic equation in the form (A10) in the ballistic graphene coincides with that in a conventional semiconductor, as it should be at large momenta.

Let us find the EF-induced modification of $G^K \equiv G^< + G^>$, disregarding the other processes, the contribution of which into the relaxation of the electron distribution, as we assumed, can be found separately. Due to the radiation some non-zero off-diagonal terms G_{ab}^K appear. In the first order in perturbation in the momentum-time representation we obtain

$$\begin{aligned}
G_{ab}^<(t_a, t_b) &= i\langle \hat{\Psi}_b^\dagger(\mathbf{p}, t_b) \hat{\Psi}_a(\mathbf{p}, t_a) \rangle \\
&\approx - \int_0^{t_b} G_{aa}^<(t_a, \tau) V_{ab}(\tau) G_{bb}^>(\tau, t_b) d\tau \\
&\quad + \int_0^{t_a} G_{aa}^>(t_a, \tau) V_{ab}(\tau) G_{bb}^<(\tau, t_b) d\tau \\
&\quad + \int_{t_a}^{t_b} G_{aa}^<(t_a, \tau) V_{ab}(\tau) G_{bb}^<(\tau, t_b) d\tau. \quad (\text{A11})
\end{aligned}$$

From now on we assume that in the vicinity of the resonance under consideration the RWA can be applied, and that the off-diagonal elements of the perturbation are taken in the form

$$V_{ab}(\tau) = W_{ab} e^{i\Omega_{ab}\tau}. \quad (\text{A12})$$

Then, from the Eq. (A11) we find in the Wigner representation

$$\begin{aligned}
G_{ab}^<(T, \mathbf{R}, \mathbf{p}, \varepsilon) &\approx \frac{2\pi W_{ab} e^{i\Omega_{ab}T}}{i(\varepsilon_a - \varepsilon_b + \Omega_{ab} - i0)} \\
&\times \left(f_b \delta\left(\varepsilon - \varepsilon_b + \frac{\Omega_{ab}}{2}\right) - f_a \delta\left(\varepsilon + \varepsilon_a - \frac{\Omega_{ab}}{2}\right) \right) \quad (\text{A13})
\end{aligned}$$

where we have introduced the total (kinetic+potential) energy ε_a of a particle with momentum \mathbf{p} and the pseudospin a and the distribution function

$$f_a(T, \mathbf{R}, \mathbf{p}) = \int \frac{d\varepsilon}{2\pi i} G_{aa}^<(T, \mathbf{R}, \mathbf{p}, \varepsilon). \quad (\text{A14})$$

Analogously,

$$\begin{aligned}
G_{ab}^>(T, \mathbf{R}, \mathbf{p}, \varepsilon) &\approx \frac{2\pi W_{ab} e^{i\Omega_{ab}T}}{i(\varepsilon_a - \varepsilon_b + \Omega_{ab} - i0)} \\
&\times \left((1 - f_a) \delta\left(\varepsilon - \varepsilon_a - \frac{\Omega_{ab}}{2}\right) \right. \\
&\quad \left. - (1 - f_b) \delta\left(\varepsilon - \varepsilon_b + \frac{\Omega_{ab}}{2}\right) \right). \quad (\text{A15})
\end{aligned}$$

Now the obtained functions $G^>$ and $G^<$ can be used to calculate the term $[\hat{V} \otimes G^K]$ in the rhs of Eq. (A10). The convolution of two functions in the Wigner representation there can be obtained following the rules formulated in the Ref. 53. For instance,

$$\begin{aligned}
V_{ba} \otimes G_{ab}^K &= e^{-\frac{i}{2} \partial_T^Y \partial^G} V_{ba} G_{ab} \\
&= V_{ba}(T) G_{ab}^K \left(\varepsilon + \frac{\Omega_{ba}}{2}, T \right). \quad (\text{A16})
\end{aligned}$$

Before substituting G^K in Eq. (A10) we integrate over the energy ε the diagonal element of this equation, in order to arrive at the kinetic equation. In that connection we also note, that the diagonal elements of the perturbation, $V_{bb}(T) = \sum_{\Omega} W_{bb}(\Omega) e^{i\Omega T}$, do not change the distribution functions f_a and thus do not enter the kinetic equation. This happens because the longitudinal

perturbation cannot change the energy level occupation. Indeed,

$$\begin{aligned}
&\int d\varepsilon [V \otimes G^K]_{bb} = \\
&\sum_{\Omega} W_{bb}(\Omega) e^{i\Omega T} \int d\varepsilon G_{bb}^K \left(\varepsilon + \frac{\Omega}{2}, T \right) - \\
&- \sum_{\Omega} W_{bb}(\Omega) e^{i\Omega T} \int d\varepsilon G_{bb}^K \left(\varepsilon - \frac{\Omega}{2}, T \right) = 0. \quad (\text{A17})
\end{aligned}$$

Keeping the second-order terms in EF or the first-order ones in the gradients of slow variables, we finally get the kinetic equation,

$$\begin{aligned}
&(\partial_T - \partial_{\mathbf{R}} U \partial_{\mathbf{p}} + v(\hat{\sigma}_z)_{bb} \partial_{\mathbf{R}}) f_b \\
&= 2\pi |W_{ba}|^2 \delta(\varepsilon_a - \varepsilon_b + \Omega_{ab}) (f_a - f_b) + (\text{St}f)_b. \quad (\text{A18})
\end{aligned}$$

Here $(\text{St}f)_b$ is the usual collision integral accounting for the change of the distribution function f_b irrespective of radiation due to impurity scattering, electron-phonon and electron-electron interactions. $(\sigma_z)_{bb} = \langle b\mathbf{p} | \hat{\sigma}_z | b\mathbf{p} \rangle$ is the direction of the particle velocity in the state with momentum \mathbf{p} and pseudospin b : (along \mathbf{p} or opposite to \mathbf{p}).

If we take the EF-induced perturbation in the form of Eq. (3.7) within the RWA in the vicinity of the corresponding resonance the kinetics of, e.g., the function $f_{\uparrow}(T, \mathbf{R}, \mathbf{p})$ is described by the equation

$$\begin{aligned}
&\left(\partial_T - \partial_{\mathbf{R}} U \partial_{\mathbf{p}} + v \frac{\mathbf{p} \partial_{\mathbf{R}}}{p} \right) f_{\uparrow} \\
&= \Gamma(\mathbf{p}) (f_{\downarrow} - f_{\uparrow}) + (\text{St}f)_b, \quad (\text{A19})
\end{aligned}$$

where

$$\Gamma(\mathbf{p}) = \frac{2\pi}{\hbar} \Delta^2 \sin^2(\widehat{\mathbf{p}}, \mathbf{E}) \delta(2vp - \hbar\Omega), \quad (\text{A20})$$

where Δ is the dynamical gap, and the Planck constant is recovered.

Equation (A19) can be understood as follows. It differs from the usual kinetic equation by the first term in the rhs describing the rate of the EF-induced change of the distribution function f_{\uparrow} . The change is due to the pseudospin flip under irradiation: $|\uparrow\rangle \rightarrow |\downarrow\rangle$ and $|\downarrow\rangle \rightarrow |\uparrow\rangle$. The rate $\Gamma(\mathbf{p})$ of both processes can be obtained from the Fermi's golden rule. Note, that neither the distribution function f_{\uparrow} nor f_{\downarrow} in Eq. (A19) is assumed to be small; the Pauli exclusion principle is taken into account in the adduced derivation or in the Fermi's golden rule, so the equation is valid for arbitrary distribution functions.

Let us examine now the applicability of our kinetic equation. Deriving the term accounting for the radiation-induced transitions, the first term in the rhs of Eq. (A18), we assumed that the distribution functions f_{\uparrow} and f_{\downarrow} are weakly perturbed by the radiation. As it follows from Eqs. (A19) and (A20), this condition is satisfied when

$$\frac{\pi \Delta^2}{\hbar v F} = \mathcal{L} \ll 1. \quad (\text{A21})$$

Indeed, if we consider the normal incidence of particles on a smooth potential barrier, using the obtained kinetic equation and setting the collision integral equal to zero, we arrive at the tunneling probability

$$T_{kinetic} = 1 - \mathcal{L}, \quad (\text{A22})$$

which agrees with the result of Eq. (3.19) in the limit $\mathcal{L} \ll 1$.

Another assumption we used when deriving the kinetic equation is that the radiation-independent relaxation processes, such as impurity scattering, electron-electron, and electron-phonon interactions weakly influence the rate of the radiation-induced transitions that can be calculated independently. If we took into account this influence, the delta-function in Eq. (A18) would have to be substituted by some function smooth on the scale \hbar/τ_R , where τ_R is some characteristic time of relaxation due to the radiation-independent processes.

Then, according to Eq. (A20), weak radiation would affect the distribution functions $f(T, \mathbf{R}, \mathbf{p})$ in the momenta interval of the characteristic width

$$\delta p \sim \frac{\hbar}{\tau_R v} \quad (\text{A23})$$

around the resonant $p_{res} = \hbar\Omega/(2v)$. For our approximation to be valid, the distribution functions in this momentum interval should be weakly changed by the radiation-independent processes. As follows from Eq. (A18), the characteristic scale, on which momentum relaxes due to these processes, is $\delta p_R \sim 1/(\tau_R F)$, where F is the characteristic slope of the potential $\partial_{\mathbf{R}}U(\mathbf{R})$ in the region under consideration. We need the fulfillment of the condition $\delta p_R \gg \delta p$ and obtain thus

$$\tau_R \gg \sqrt{\frac{\hbar}{vF}}. \quad (\text{A24})$$

Under this condition the radiation-induced transitions, described by the first term in the rhs of Eq. (A18), can be considered independently of the other processes described by the second term there.

-
- ¹ K. S. Novoselov, A. K. Geim, S. V. Morozov, D. Jiang, Y. Zhang, S. V. Dubonos, I. V. Grigorieva, and A. A. Firsov, *Science* **306**, 666 (2004).
- ² P. R. Wallace, *Phys. Rev.* **71**, 622 (1947).
- ³ A. K. Geim and K. S. Novoselov, *Nature Mat.* **6**, 183 (2007).
- ⁴ S. V. Morozov, K. S. Novoselov, F. Schedin, D. Jiang, A. A. Firsov, and A. K. Geim, *Phys. Rev. B* **72**, 201401(R) (2005).
- ⁵ K. S. Novoselov, A. K. Geim, S. V. Morozov, D. Jiang, M. I. Katsnelson, I. V. Grigorieva, S. V. Dubonos, and A. A. Firsov, *Nature* **438**, 197 (2005).
- ⁶ Y. Zhang, Y.-W. Tan, H. L. Stormer, and P. Kim, *Nature* **438** (2005).
- ⁷ A. Das, S. Pisana, B. Chakraborty, S. Piscanec, S. K. Saha, U. V. Waghmare, K. S. Novoselov, H. R. Krishnamurthy, A. K. Geim, A. C. Ferrari, et al., *Nat. Nanotechnol.* **3**, 201 (2007).
- ⁸ S. V. Morozov, K. S. Novoselov, M. I. Katsnelson, F. Schedin, D. C. Elias, J. A. Jaszczak, and A. K. Geim, *Phys. Rev. Lett.* **100**, 016602 (2008).
- ⁹ Y. Q. Wu, P. D. Ye, M. Capano, Y. Xuan, Y. Sui, M. Qi, and J. Cooper, *Appl. Phys. Lett.* **92**, 092192 (2008).
- ¹⁰ K. I. Bolotin, K. J. Sikes, Z. Jiang, G. Fudenberg, J. Hone, P. Kim, and H. L. Stormer, *arXiv e-prints* (2008), 0802.2389.
- ¹¹ M. C. Lemme, T. J. Echtermeyer, M. Baus, and H. Kurz, *IEEE Electron Device Lett.* **28**, 282 (2007).
- ¹² B. Huard, J. A. Sulpizio, N. Stander, K. Todd, B. Yang, and D. Goldhaber-Gordon, *Phys. Rev. Lett.* **98**, 236803 (2007).
- ¹³ J. R. Williams, L. DiCarlo, and C. M. Marcus, *Science* **317**, 638 (2007).
- ¹⁴ B. Özyilmaz, P. Jarillo-Herrero, D. Efetov, D. A. Abanin, L. S. Levitov, and P. Kim, *Phys. Rev. Lett.* **99**, 166804 (2007).
- ¹⁵ Z. Chen, Y.-M. Lin, M. J. Rooks, and P. Avouris, *Physica E* **40**, 228 (2007).
- ¹⁶ R. V. Gorbachev, A. S. Morozov, A. K. Savchenko, D. W. Horsell, and F. Guinea, *arXiv e-prints* (2008), 0804.2081.
- ¹⁷ G. Liu, J. Valesco Jr., W. Bao, and C. N. Lau, *arXiv e-prints* (2008), 0804.2513.
- ¹⁸ G. W. Semenoﬀ, *Phys. Rev. Lett.* **53**, 2449 (1984).
- ¹⁹ F. D. M. Haldane, *Phys. Rev. Lett.* **61**, 2015 (1988).
- ²⁰ M. I. Katsnelson, K. S. Novoselov, and A. K. Geim, *Nature Phys.* **2**, 620 (2006).
- ²¹ X. Duan, Y. Huang, Y. Cui, J. Wang, and C. M. Lieber, *Nature* **409**, 66 (2001).
- ²² M. S. Marcus, J. M. Simmons, O. M. Castellini, R. J. Hammers, and M. A. Eriksson, *J. Appl. Phys.* **100**, 084306 (2006).
- ²³ M. Freitag, Y. Martin, J. A. Misewich, R. Martel, and P. Avouris, *Nano Lett.* **3**, 1067 (2003).
- ²⁴ Y. Ohno, S. Kishimoto, T. Mizutani, T. Okazaki, and H. Shinohara, *Appl. Phys. Lett.* **84**, 1368 (2004).
- ²⁵ J. Wang, M. S. Gudiksen, X. Duan, Y. Cui, and C. M. Lieber, *Science* **293**, 1455 (2001).
- ²⁶ P. Hänggi, in *Quantum transport and dissipation*, edited by T. Dittrich, P. Hänggi, G.-L. Ingold, B. Kramer, G. Schön, and W. Zwerger (Wiley-VCH, Weinheim, 1998).
- ²⁷ V. M. Galitskii, S. P. Goreslavskii, and V. F. Elesin, *Sov. Phys. JETP* **30**, 117 (1970).
- ²⁸ V. F. Elesin, *Sov. Phys. Semicond.* **4**, 1302 (1970).
- ²⁹ V. F. Elesin, *Sov. Phys. Semicond.* **11**, 1470 (1970).
- ³⁰ V. F. Elesin, *Sov. Phys. JETP* **32**, 328 (1971).
- ³¹ V. F. Elesin, A. I. Erko, and A. I. Larkin, *JETP Lett.* **29**,

- 651 (1979).
- ³² Q. T. Vu, H. Haug, O. D. Mücke, T. Tritschler, M. Wegener, G. Khitrova, and H. M. Gibbs, *Phys. Rev. Lett.* **92**, 217403 (2004).
- ³³ S. P. Goreslavskii and V. F. Elesin, *JETP Lett.* **10**, 316 (1969).
- ³⁴ A. S. Alexandrov and V. F. Elesin, *Sov. Phys. JETP* **35**, 403 (1972).
- ³⁵ T. J. Inagaki and M. Aihara, *Phys. Rev. B* **66**, 075204 (2002), and references therein.
- ³⁶ M. V. Fistul and K. B. Efetov, *Phys. Rev. Lett.* **98**, 256803 (2007).
- ³⁷ M. Moskalets and M. Büttiker, *Phys. Rev. B* **66**, 205320 (2002).
- ³⁸ E. J. Mele, P. Král, and D. Tománek, *Phys. Rev. B* **61**, 7669 (2000).
- ³⁹ L. Allen and J. H. Eberly, *Optical resonance and two-level atoms* (Dover, New-York, 1975).
- ⁴⁰ E. O. Kane and E. I. Blount, in *Tunneling Phenomena in Solids*, edited by E. Burstein and S. Lundqvist (Plenum Press, New York, 1969).
- ⁴¹ V. V. Cheianov and V. I. Fal'ko, *Phys. Rev. B* **74**, 041403(R) (2006).
- ⁴² A. V. Shytov, N. Gu, and L. S. Levitov, arXiv e-prints (2008), 0708.3081.
- ⁴³ M. V. Fistul and K. B. Efetov, *Phys. Rev. B* **76**, 195329 (2007).
- ⁴⁴ L. M. Zhang and M. M. Fogler, *Phys. Rev. Lett.* **100**, 116804 (2008).
- ⁴⁵ M. Abramowitz and I. A. Stegun, eds., *Handbook of Mathematical Functions with Formulas, Graphs, and Mathematical Tables* (U.S. Government Printing Office, 1972), 10th ed.
- ⁴⁶ M. M. Fogler, D. S. Novikov, L. I. Glazman, and B. I. Shklovskii, *Phys. Rev. B* **77**, 075420 (2008).
- ⁴⁷ I. L. Aleiner and K. B. Efetov, *Phys. Rev. Lett.* **97**, 236801 (2006).
- ⁴⁸ E. G. Mishchenko, *Phys. Rev. Lett.* **98**, 216801 (2007).
- ⁴⁹ J. M. Dawlaty, S. Shivaraman, M. Chandrashekar, F. Rana, and M. G. Spencer, *Appl. Phys. Lett.* **92**, 042116 (2008).
- ⁵⁰ K. Henneberger, *Physica A* **150**, 419 (1988).
- ⁵¹ K. Henneberger and H. Haug, *Phys. Rev. B* **38**, 9759 (1988).
- ⁵² F. Jahnke and K. Henneberger, *Phys. Rev. B* **45**, 4077 (1992).
- ⁵³ J. Rammer and H. Smith, *Rev. Mod. Phys.* **58**, 323 (1986).